FACULDADE DE ENGENHARIA DA UNIVERSIDADE DO PORTO

Role of SPARC derived peptides on endothelial/prostate cancer cells monoculture and co-culture models

Francisca Maria Rocha Moreira de Soares Seabra

Mestrado Integrado em Bioengenharia

Supervisor: Professor Susana R. Sousa

Co-supervisor: Professor Carmen Jerónimo

31st January 2020

Role of SPARC derived peptides on endothelial/prostate cancer cells monoculture and co-culture models

Francisca Maria Rocha Moreira de Soares Seabra

Mestrado Integrado em Bioengenharia

31st January 2020

This thesis was supervised by:

Professor Susana Maria Ribeiro e Sousa Mendes de Freitas (supervisor)

Instituto Superior de Engenharia do Porto, Instituto Politécnico do Porto, Portugal

i3S – Instituto de Investigação e Inovação em Saúde, Universidade do Porto, Portugal

INEB – Instituto de Engenharia Biomédica, Universidade do Porto, Portugal

Professor Carmen de Lurdes Fonseca Jerónimo (co-supervisor)

Instituto de Ciências Biomédicas Abel Salazar, Universidade do Porto, Portugal

CI-IPO Porto – Centro de Investigação do Instituto Português de Oncologia do Porto, Portugal

Institution where this dissertation was performed:

i3S – Instituto de Investigação e Inovação em Saúde, Universidade do Porto, Portugal

INEB – Instituto de Engenharia Biomédica, Universidade do Porto, Portugal

CI-IPO Porto – Centro de Investigação do Instituto Português de Oncologia do Porto, Portugal

Para os meus avôs, o Jorge e a Jonita.

Abstract

Prostate cancer (PCa) is the second most incident cancer in men worldwide. PCa is characterised for developing bone metastases in most aggressive cases and when it does, it becomes an incurable disease. SPARC (secreted protein, acidic and rich in cysteine) is an extracellular protein that has been proved to have a role in bone remodelling, angiogenesis and cancer-related processes, namely in PCa, however, its exact interaction mechanisms are not yet defined. Thus, it is possible to formulate that SPARC may have a relevant role in PCa bone metastization.

The aim of this work was to investigate how SPARC influences PCa angiogenesis and bone metastization. This was achieved by developing monocultures and co-cultures of PCa (LNCaP and PC-3) and endothelial (HPMEC-ST1.6R) cell lines, in a type I collagen and hydroxyapatite biocomposite functionalised with different concentrations of SPARC and SPARC peptides; namely, SPARC 2.3 peptide, that stimulates endothelial cell proliferation and angiogenesis, and SPARC 4.2 peptide that has the opposite effect on proliferation but stimulates endothelial cell migration.

Metabolic activity was access through a resazurin assay, for a 5 days monocultures, with a single concentration of SPARC (0.23 μM) and SPARC 2.3 peptide (23 μM). When compared with the biomaterial, HPMEC-ST1.6R showed an increase in both cases, PC-3 showed a null influence and LNCaP showed a decrease in proliferation for SPARC, but an increase for SPARC 2.3 peptide. Endothelial cells metabolic activity was also accessed for SPARC 4.2 peptide concentration optimization: from four different concentrations, a 230 μM concentration was elected for leading to the highest proliferation inhibition.

Epithelial-mesenchymal transition (EMT) is a process related to angiogenesis that also plays an important part in tumour invasion and metastization. The gene expression of EMT related genes was assessed through real-time reverse transcription polymerase chain reaction, for both monocultures and endothelial/PCa co-cultures, with SPARC (0.23 μM and 0.69 μM) and SPARC 2.3 peptide (23 μM). The results revealed that the used biomaterial induces a mesenchymal phenotype expression in HPMEC-ST1.6R when compared with a positive control. However, epithelial phenotype seems to be promoted with the addition of SPARC and SPARC 2.3 peptide, for all the 3 cell lines and for the HPMEC-ST1.6R/PC-3 co-culture. Regarding the HPMEC-ST1.6R/LNCaP co-culture, the results were inconclusive.

Lastly, it was performed an immunostaining protocol with biomarkers monoclonal CD31, for the endothelial cells, and alpha-methylacyl-coA racemase (AMACR), for the PCa cells. Both were tested for the concentration and specificity, in order to establish in the future a protocol to access cell morphology in endothelial/PCa co-cultures. The antibody monoclonal CD31 revealed to be adequate for identifying unequivocally endothelial cells, however further work needs to be done regarding the PC-3 line.

To sum it up, the results showed that although SPARC addition lead to endothelial cell proliferation, it also induced a mesenchymal phenotype for all cell lines, which can be associated with a low migration potential, indicating that SPARC may be a potential path to a bone metastatic PCa inhibitory therapy. All the results obtained, including the preliminary results for immunostaining,

confirmed that the developed *in vitro* model is and adequate way to continue exploring SPARC behaviour.

Resumo

O cancro da próstata (CaP) é o segundo cancro com maior incidência em homens, a nível mundial. Em casos mais graves, este cancro caracteriza-se pelo desenvolvimento de metástases no osso, sendo atualmente incurável. A SPARC (*secreted protein, acidic and rich in cysteine*) é uma proteína extracelular que influencia processos envolvendo formação de osso, angiogénese e cancro, nomeadamente CaP, no entanto os seus mecanismos de interação não estão ainda completamente definidos. Desta forma é possível afirmar que a SPARC poderá ter um papel importante na metastização óssea do CaP.

O objetivo deste trabalho é investigar a influência da SPARC na metastização óssea e angiogénese do CaP. Este será atingido através do desenvolvimento de monoculturas e co-culturas de células de CaP (LNCaP e PC-3) e endoteliais (HPMEC-ST1.6R), usando como suporte um biocompósito de colagénio tipo I e hidroxiapatite, funcionalizado com diferentes concentrações de SPARC e seus péptidos; nomeadamente, o péptido 2.3, que estimula a proliferação de células endoteliais e angiogénese, e o péptido 4.2, que tem o efeito oposto mas estimula a migração das mesmas.

Foi avaliada atividade metabólica através de um ensaio de resazurina, para monoculturas de 5 dias, com uma concentração única de SPARC (0.23 μM) e péptido 2.3 (23 μM). Comparando com biomaterial apenas, HPMEC-ST1.6R apresentou um aumento para ambos os casos, PC-3 apresentou influência nula e LNCaP uma diminuição para a SPARC, mas um aumento na proliferação para o péptido 2.3. A atividade metabólica de células endoteliais foi também avaliada para otimizar a concentração do péptido 4.2: de 4 diferentes concentrações, foi escolhida uma concentração de 230 μM por corresponder à maior diminuição da proliferação.

A transição epitelial-mesenquimal (TEM) é um processo relacionado com a angiogénese que também desempenha um papel importante na invasão e metastização de tumores. A expressão génica de genes relacionados com a TEM foi avaliada através de um RT-PCR (*reverse transcription polymerase chain reaction*) em tempo real, para monoculturas e co-culturas, com SPARC (0.23 μM e 0.69 μM) e péptido 2.3 (23 μM). Os resultados demonstraram que o biomaterial em estudo induz um fenótipo mesenquimal na linha HPMEC-ST1.6R, quando comparado com um controlo positivo. No entanto, um fenótipo endotelial parece ser induzido com a adição de SPARC e péptido, para as 3 linhas celulares e co-culturas de HPMEC-ST1.6R/PC-3. Os resultados foram inconclusivos para a co-cultura de HPMEC-ST1.6R/LNCaP.

Por fim, foi realizado um procedimento de imunocoloração com os marcadores CD31 monoclonal, para as células endoteliais, e alfa-metilacil-coA racemase (AMACR), para as células do CaP. Ambos foram testados para concentrações e especificidade, com o objetivo de estabelecer um futuro protocolo para visualizar a morfologia celular em co-culturas. O anticorpo CD31 monoclonal revelou-se uma escolha adequada para a identificação inequívoca das células endoteliais, no entanto, é necessário continuar a investigar a coloração da linha PC-3.

Em suma, os resultados mostraram que, apesar da adição de SPARC conduzir à proliferação de células endoteliais, um fenótipo epitelial foi induzido para todas as linhas celulares, fenómeno

que pode ser associado a um baixo potencial de migração, indicando que a SPARC poderá ser um potencial caminho para estabelecer uma terapia inibitória da metastização do CaP no osso. Todos os resultados obtidos, incluindo os resultados preliminares de imunocoloração, confirmam que o modelo *in vitro* desenvolvido é um meio adequado para continuar a explorar o comportamento da SPARC.

Agradecimentos

Em primeiro lugar, gostava de agradecer a todos os que trabalharam comigo e me ajudaram nesta jornada de quase dois anos que chega agora a um fim. Em particular, gostava de agradecer às minhas orientadoras: à Professora Doutora Susana R. Sousa e à Professora Doutora Carmen Jerónimo. Obrigada por toda a orientação, paciência e disponibilidade e por tudo o que me ensinaram sobre ciência e trabalho. Gostava de deixar também um agradecimento ao Professor Doutor Fernando Jorge Monteiro por me ter dado a oportunidade de conhecer e me juntar a este projeto. Trabalhar num tema tão importante para a vida de tantos, e em especial ter tido a motivação de trabalhar dentro de uma instituição como o IPO-Porto, mudou para sempre a minha visão do mundo, e por isso, estarei sempre grata aos três.

Gostava de agradecer à Nilza Ribeiro e à Vera Miranda-Gonçalves, por todo o treino, orientação e apoio, por estarem sempre disponíveis para qualquer dúvida, mas principalmente por tudo o que aprendi com ambas e irei carregar comigo ao longo da minha vida profissional.

Gostava de agradecer às minhas colegas, que me acompanharam durante o meu tempo no i3S. À Sofia Sousa, que será para sempre a minha primeira amiga e colega de laboratório. À Luisamaria Matiz e à Helena Branco, a quem tive o prazer de acompanhar e, espero, ensinar algo. A todas desejo as máximas felicidades na vossa vida académica e profissional.

Obrigada a todos os que fizeram e fazem parte dos grupos Biocomposites e Epigenética e Biologia do Cancro. Obrigada por me terem acolhido tão bem nas vossas "casas" e por me terem feito parte da família. Obrigada pelos bons momentos, pelo apoio e por tudo o que me ensinaram.

Gostava também de agradecer a todas as pessoas e projetos que, durante os meus 5 anos na FEUP e no ICBAS, de uma maneira ou outra, me inspiraram e apoiaram como estudante e me ajudaram a ganhar o gosto pela ciência e pela Engenharia. Em particular, obrigada a todos os colegas que se tornaram amigos; obrigada por todas as boleias, todas as noitadas de estudo ou não, todos os desesperos e conquistas, mas principalmente, obrigada pelo sentimento de pertença a algo maior, que levo comigo para outras paragens.

Numa nota mais pessoal, gostava de agradecer aos meus pais, mesmo que eles me tenham dito que não queriam que o fizesse. Obrigada por me terem criado para ser a mulher que sou hoje e por nunca me terem desencorajado de seguir aquilo que queria. Gostava também de agradecer a todos amigos que são neste momento para mim como família, sejam eles conquistadores de terras alentejanas ou partes essenciais para a sobrevivência da célula. Obrigada por terem estado sempre ao meu lado, nos bons e nos maus momentos, por me aceitarem como sou, e terem efetivamente feito destes anos os melhores anos da minha vida.

E por falar em grandes influências, gostava de terminar a agradecer a todos os Gambozinos por este país e mundo fora. Obrigada por me terem ensinado que apesar de no fundo sermos todos Anas que querem nunca ter saído da barriga da mãe, através da música e cultura, de muito trabalho mas também imaginação, podemos conquistar este mundo com tantas maneiras de ver e viver.

Francisca

Adeus, ó pedras do Porto,
tão frias, pela manhã,
eu vou partir num comboio
na estação de Campanhã.

Adeus, ó sinos da Sé,
Vendedeiras do Bolhão,
Adeus ó fogo em que ardi
Na noite de S. João.

Adeus, ó verde cavalo
Da Praça da Liberdade
E Douro que me douraste
Os sonhos de cada idade.

Ai, como pesa a saudade
numa mochila vazia…
Eu vou para o fim do mundo
Mas hei-de voltar um dia.

Luísa Ducla Soares. O Emigrante (Campanhã). In *Com Quatro Pedras na Mão*

Contents

List of Figures

List of Tables

Abbreviations and Symbols

aa	amino acids
AMACR	Alpha-Methylacyl-CoA Racemase
β-GUS	β-glucuronidase
BSA	Bovine Serum Albumin
CD31	Cluster of Differentiation 31
CDH1	Cadherin
CDH2	Cadherin 2
cDNA	complementary Deoxyribonucleic Acid
col-I	type I collagen
CT	COOH-terminal
DDR1	Discoidin Domain Receptor 1
ECM	Extracellular Matrix
EMT	Epithelial-Mesenchymal Transition
FBS	Foetal Bovine Serum
FS	Follistatin-like
HA	Hydroxyapatite
HPMEC-ST1.6R	Human Pulmonary Microvascular Endothelial Cells ST1.6R
i3S	Instituto de Investigação e Inovaçao em Saúde
IFM	Inverted Fluorescence Microscope
INEB	Instituto de Engenharia Biomédica
IPO	Instituto Português de Oncologia
LCSM	Laser Confocal Scanning Microscope
LNCaP	Lymph Node Carcinoma of the Prostate
MET	Mesenchymal-Epithelial Transition
nanoHA	nanophased Hydroxyapatite
NT	NH_2-terminal
PBS	Phosphate Buffered Saline
PCa	Prostate Cancer
PCR	Polymerase Chain Reaction
PDL	Poly-D-lysine
PSA	Prostate-Specific Antigen
qPCR	quantitative Polymerase Chain Reaction
RFU	Reference Fluorescence Units
RNA	Ribonucleic Acid
rpm	rotations per minute
RT	Reverse Transcription
RT-PCR	Reverse Transcription Polymerase Chain Reaction
SEM	Scanning Electron Microscopy
SPARC	Secreted Protein, Acidic and Rich in Cysteine
VIM	Vimentin
ZEB1	Zinc finger E-box-Binding homeobox 1

Chapter 1

Introduction

1.1 Context

Cancer is the term used for defining a group of diseases characterised by uncontrolled growth and spread of abnormal cells, caused by genetic mutations. There are 5 main types of cancer, according to where the mutation occurs [1]:

- **carcinoma**: epithelial cell cancer. It is the most common type of cancer. There are different subtypes, including adenocarcinoma (derived from glandular epithelium), basal cell carcinoma, squamous cell carcinoma and transitional cell carcinoma;
- **sarcoma**: connective tissues cancer, such as bone, cartilage, fat, muscle or blood vessels. They are normally divided into 2 main types: bone sarcomas (osteosarcomas) and soft tissue sarcomas;
- **leukaemia**: bone marrow cancer. The most common type of cancer in children;
- **lymphoma and multiple myeloma**: immune system cells cancer (lymph and plasma cells);
- **brain and spinal cord cancers**: central nervous system cancer.

The prostate gland is a male reproductive organ, with the size of a chestnut, located between the bladder neck and the rectal ampulla, crossed by the urethra and the ejaculatory duct (Figure 1.1a). Its function is to secrete the prostatic fluid [2].

Prostate cancer (PCa) is a cancer that starts with the mutation of prostate cells (Figure 1.1b). The most common type of PCa is adenocarcinoma. Other types include sarcomas, small cells carcinomas, neuroendocrine tumours and transitional cell carcinomas [3].

Cancer cells do not adhere and form tissues in the same way normal human cells do, since they establish weaker intercellular connective forces. Under the presence of certain signalling factors, this allows cancer cells to travel to secondary sites, in a phenomenon called invasion, adhere and form new tumours, by a process that receives the name of metastization. A tumour in the site

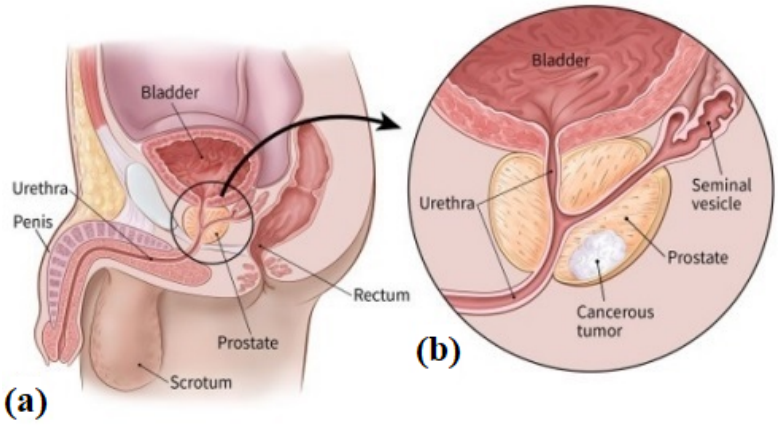

Figure 1.1: The prostate gland. (a) Localization of the prostate in the male reproduction system. (b) A more detailed view of the beginning of PCa. Adapted from [3].

where cancer starts is called a primary tumour; when it spreads to other parts of the body it results in a secondary tumour or metastasis [1].

A cancer staging system is a systematic way to describe how far cancer has spread. PCa has 4 main stages, with some stages further divided. The scale starts with stage I, where PCa is confined to the prostate, and goes to stage IVB, where PCa can be present in the tissue near the prostate, nearby lymph nodes and other parts of the body, such as distant lymph nodes, bones and other organs [3].

PCa bone metastases occur mainly in sites where a large amount of red bone marrow is present, such as the vertebral column, pelvis, ribs and long bones. The interaction between the metastasis and the bone stroma interferes with bone remodelling and has as consequence biomechanical instability that leads to pathological fractures. This increases with the size of the tumour, provoking compression and pain and also impairing the haematologic production [4, 5].

Guidelines for treating bone metastases include preventative treatment for fractures, pain control and slowing the spread of the cancer [3]. However, there is a lack of approved bone-targeted therapies. The exact mechanism of bony metastases formation is not even conclusively defined [4].

1.2 Motivation

In 2018, there were 18.1 million new cases of cancer worldwide, making cancer the second leading cause of death globally, with an estimated 9.6 million deaths [6]. In Portugal, 58 199 new cases were registered, leading to 28 960 deaths in that same year [7].

Worldwide, PCa represents 7.1% of the new cases and 3.8% of the deaths. This makes PCa the fourth most incident cancer, for both sexes, and the second most incident and the fifth leading cause of death, for men only [6]. In Portugal, in 2018, 1 879 cases of death were registered, representing 18.3 in 100 000 inhabitants [7].

The 5-year relative survival rate for men diagnosed with PCa, for all stages of cancer, is currently 99%, but this fact has to be carefully taken into consideration: for local or regional stages, the survival rate is higher than 99%, but for distant stages, it drops to 29% [8]. This is due to the fact that metastization in bone occurs in nearly 80% of the cases of metastatic PCa [4]; in fact, in one autopsy study of 1 589 patients, approximately 90% of the ones whose cause of death was PCa hematogenous metastases were diagnosed with bone metastases [9]. This way, it is possible to conclude that in order to reduce the mortality associated with PCa, it is crucial to understand the mechanism that leads to osseous metastization and propose new therapies.

Furthermore, Crawford *et al.* [10] states that there is a need for biomarkers for PCa: there is the lack of a test or biomarker that might identify not only the presence of PCa but also its stage. Existing solutions, as the prostate-specific antigen (PSA), have limitations, namely at the specificity level, leading to false positives and false negatives. A new biomarker could help reduce the number of unnecessary biopsies or help to stage the disease and classifying its extent, leading to informed treatment decisions from both patients and physicians.

1.3 Aim of the work

SPARC (secreted protein, acidic and rich in cysteine), also known as osteonectin or Basement-Membrane Protein 40, is a matricellular protein that is found in the extracellular matrix (ECM) of both bone and multiple tumour types, including PCa. SPARC has been reported to be associated with tissue remodelling and may also have a role in the growth and progression of tumours, concretely, in bone metastasis. However, the exact way of how SPARC interacts in these mechanisms is not yet defined [11].

It is possible to formulate that SPARC may be a key element to understand the PCa metastization process, a potential biomarker and even be a path to a new treatment.

The aim of this work is to better understand SPARC influence in mechanisms that occur in tumorigenesis and PCa osseous metastization. *In vitro* monoculture and co-culture models were developed in a bone biomimetic biomaterial, fabricated following the protocol presented in Ribeiro *et al.* [12] and functionalised with SPARC and SPARC derived peptides. Results of cell metabolic activity, proliferation, morphology and expression of some genes of interest will be presented and discussed.

1.4 Structure

This document is structured in the following way: Chapter 2 contains a literature review in: 1) cancer angiogenesis and related phenomena, 2) osseous metastization, bone structure and biomimetic materials, 3) relevant cell lines and 4) SPARC and its influence in PCa and the aforementioned mechanisms. The state of the art is analysed, regarding used experimental models, major results and conclusions.

Chapter 3 presents the materials and followed methodology regarding biomaterial fabrication, cell culture models, metabolic assays, gene expression and cell morphology assessment.

The results of the experiences conducted are described in Chapter 4. Chapter 5 further analyses these results, comparing it with previously conducted work and the state of the art.

Chapter 6 comprises a brief summary of the main conclusions of the work exposed and Chapter 7 explores future lines of investigation regarding the same topics exposed in this dissertation.

1.5 Principal contributions

The manufacturing procedure was conducted by the author at Instituto de Engenharia Biomédica (INEB)/Instituto de Investigação e Inovação em Saúde (i3S), with the supervision of Nilza Ribeiro, PhD. Scanning electron microscopy was performed at Centro de Materiais da Universidade do Porto, by technicians Rui Rocha, MSc, and Daniela Silva, BSc.

Cell culture experiences were conducted by the author at INEB/i3S, with the collaboration of Sofia Sousa, BSc, Luisamaria Matiz, BSc, and Helena Branco, BSc. SPARC 4.2 and 2.3 peptides were synthesized and purified at REQUIMTE – Laboratório Associado para a Química Verde, by Sofia Sousa and Helena Branco, respectively.

Protocols for assessing gene expression were conducted by the author at Instituto Português de Oncologia (IPO) Porto Research Centre, with the supervision of Vera Miranda-Gonçalves, PhD.

The immunostaining protocol was optimized and implemented by the author, both in INEB/i3S and IPO Porto Research Centre. Inverted fluorescence microscopy and laser confocal scanning microscopy were conducted at i3S, technically assisted by Dalila Pedro, PhD, and Maria Gómez Lázaro, PhD, respectively. Hence, the author acknowledges the support of the i3S Scientific Platform Bioimaging, member of the national infrastructure PPBI - Portuguese Platform of Bioimaging (PPBI-POCI-01-0145-FEDER-022122).

Chapter 2

Literature review

2.1 Angiogenesis in cancer

Angiogenesis and vasculogenesis are the processes that lead to the formation of new blood vessels. In angiogenesis, a previously existing vessel is used whereas, in vasculogenesis, blood vessels are formed *de novo* by differentiation from endothelial progenitor cells. Lymphangiogenesis is the process that leads to lymphatic vessels formation. All these processes are necessary for cell survival since they lead to the formation of a vascular network, that allows the necessary transport to acquire nutrients and oxygen and to dispose carbon dioxide and waste products.

Like any other cells, developing a vasculature is mandatory for cancer cells. It has been proved that the growth of localised tumours beyond 1-2 mm^3 in volume requires angiogenesis. This makes angiogenesis a hallmark of cancer, being a crucial factor in metastization. Highly vascular tumours can be related to a higher probability of developing metastases and poorer prognoses.

The growth of blood vessels can be described in the following steps:

- segregation of proteases that digest the vascular basement membrane, allowing endothelial cells migration;
- segregation of angiogenic factors that activate endothelial cells, leading to their migration;
- proliferation of the endothelial cells, secreting new vascular basement membrane and forming new vessels.

Angiogenesis is regulated by the presence of activator and inhibitor molecules. This is called the angiogenic switch: there is a balance between proangiogenic and antiangiogenic substances, occurring a switch when this balance is disturbed by either an increase or a decrease of proangiogenic and antiangiogenic factors. In cancer, there is in simultaneous an upregulation of proangiogenic factors and a downregulation of antiangiogenic factors. Unlike normal cells, the balance is not restored after the formation of the blood vessels, leading to continuous angiogenesis that gives origin to new tortuous tumour vessels [13–15].

2.1.1 Epithelial-mesenchymal transition (EMT)

A chaotic vessel architecture, caused by continuous angiogenesis, results in disturbances in the blood flow that lead to intermittent hypoxia. In carcinomas, hypoxia has been associated with increasingly invasive tumours and occurrence of epithelial-mesenchymal transition (EMT) of tumour cells [13].

EMT is a process that allows an epithelial cell to undergo multiple biochemical changes and assume a mesenchymal cell phenotype. Epithelial cells show apical-basal polarity, intercellular junctions (that allow adhesion and communication with other cells in the tissue) and interaction with a basement membrane via its basal surface. On its hand, a mesenchymal cell has enhanced migratory capacity and invasiveness, elevated resistance to apoptosis, and considerably increased production of ECM components. Epithelial cells typically exert a tissue-specific function, while mesenchymal cells play a supporting role.

EMT starts with several distinct molecular processes, such as activation of transcription factors, expression of several proteins, production of ECM-degrading enzymes and alterations in the expression of certain microRNAs. During EMT, epithelial cells lose their junctions and polarity, reorganize their cytoskeleton, redefine cell shape and reprogramme gene expression. Additionally, these cells acquire resistance to senescence and apoptosis. The process is only complete with the degradation of the underlying basement membrane.

Depending on the environment, the epithelial cells that undergo these processes may acquire only some characteristics of the mesenchymal phenotype: this is called a partial EMT. EMT is currently called a "transition" because there is the occurrence of the reverse process: mesenchymal-epithelial transition (MET).

There are 3 types of EMT: type 1 EMT is associated with embryonic processes, type 2 EMT is related to inflammation and fibrosis and type 3 EMT is related to tumour growth and cancer invasion (Figure 2.1a). More specifically, type 3 EMT occurs in cells that have previously suffered genetic alterations. It is believed that carcinoma cells undergoing a type 3 EMT is a key for the beginning of the metastization process and a consequence of several signalling agents, generating cells with invasive properties. It is also believed that MET allows the formation of a secondary tumour. These phenomena are controlled by the microenvironment, namely, the absence of the signals that triggered the EMT in the first place leads to MET and metastasis formation [16, 17].

2.1.2 Genes involved in EMT and metastization

Cadherin 1 (CDH1), also known as epithelial cadherin or E-cadherin, is a protein responsible for the stability of epithelial cell-cell adhesive junctions and maintaining apico-basal cell polarity and epithelial tissue structure. This way, CDH1 plays an important role in epithelial cells and EMT only occurs with a decrease of *CDH1* gene expression. In cancer, this decrease plays a crucial role, since it enables the release of cancer cells from the primary tumour.

In fact, there is a "cadherin switch" during EMT: *CDH1* low expression is followed by an up-regulation or *de novo* expression of cadherin 2 (CDH2). CDH2, also known as neural cadherin

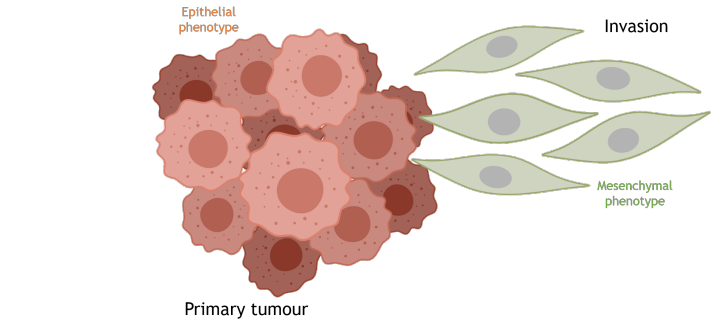

(a)

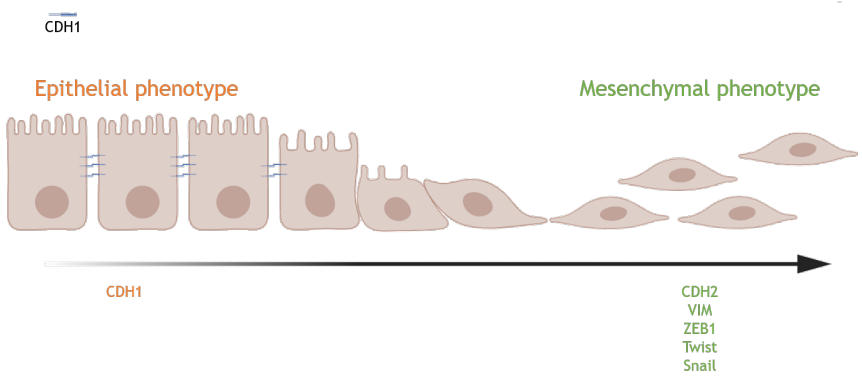

(b)

Figure 2.1: Epithelial-mesenchymal transition. (a) Type 3 EMT: EMT that enables invasion and metastasis. (b) Progressive transition of epithelial markers to mesenchymal markers, leading to a phenotype transition. Created with www.BioRender.com

or N-cadherin, is a protein responsible for cell-cell adhesion during migration since collective cell migration facilitates the invasion of epithelial cells. This means that CDH2 plays an active role in the promotion of the metastatic capacity of tumour cells and can be correlated with poorer prognosis [18].

Vimentin (VIM) is a protein of the intermediate filament family and is regarded as a mesenchymal marker. Its functions are maintaining cellular integrity and provide resistance against stress. The increase of *VIM* expression is related with EMT occurrence but also with increased tumour growth, invasion and poor prognosis [19]: during EMT, VIM interacts with motor proteins, leading to changes in the composition of the intermediate filament, enabling cell mobility [17].

Zinc finger E-box-binding homeobox 1 (ZEB1) is an EMT-inducing transcription factor. The expression of *ZEB1* leads to the repression of *CDH1*, by binding to two E-box sequences in its promoter region. With repression of *CDH1*, the epithelial phenotype is repressed and mesenchymal genes and *CDH2* are activated, promoting EMT and tumour invasiveness [17, 20].

Twist is also a transcription factor that plays a role in EMT, being *TWIST1* the gene for Twist. When activated, Twist downregulates *CDH1* and upregulates *CDH2*, independently of Snail. Its gene expression also can be related to *SPARC* activation and *ZEB1* induction, in cooperation with

Snail. *TWIST1* is expressed in the presence of hypoxia and its deregulation has been related to several types of cancer [17, 21].

On its hand, Snail is another EMT-related transcription factor, encoded by the *SNAI1* gene, that represses *CDH1* and activates *CDH2* and *VIM*. Its expression is induced by the presence of cellular reactive oxygen species, formed by other mechanisms that occur during EMT [17, 22].

In short, a high expression of *CDH2*, *VIM*, *ZEB1*, *TWIST1* and *SNAI1* and low expression of *CDH1* are good indicators of EMT potential, cell invasion and therefore tumour metastization (Figure 2.1b).

Lastly, the discoidin domain receptor 1 (DDR1) also plays an important role in metastization. *DDR1* is primarily expressed in epithelial cells, being responsible for the stabilisation of CDH1 in the cell membrane, leading to epithelial differentiation. This means that normally, subexpression of *DDR1* leads to EMT. However, *DDR1* appears to be overexpressed in several types of cancers. One explanation is that *DDR1* may be overexpressed in non-EMT metastization since it promotes collective migration of epithelial cells [23].

Another explanation is related to the fact that DDR1 binds and gets activated by collagens, including type I collagen (col-I): the overexpression of *DDR1* alters the ECM environment and enables metastasis [24]. According to Shimada *et al.* [25], *DDR1* is overexpressed in PCa cells, like LNCaP, and its downregulation suppresses cancer invasion and cell survival.

2.2 Bone metastases in prostate cancer

As previously mentioned, the exact mechanism of the formation of PCa bone metastases is not yet completely defined. One theory is the "seed and soil" hypothesis: the "seed" is the metastatic cells and the "soil" is the microenvironment. After the angiogenic and growth factors release, individual PCa cells detach from the primary tumour by EMT and invade through the stromal tissue into the vascular system. When cells reach the cortical or medullary bone, PCa cells interact with the bone microenvironment, more precisely, with specific receptors, growths factor and bone-derived proteins, and establish micrometastases. After this, the tumour modifies its immediate environment and angiogenesis comes into the play, in order to allow tumour survival, growth and further expansion to other sites [4, 26].

Regarding the above-mentioned growth factors and other signalling molecules, it is possible to find a very complex scheme of interactions, as it is possible to partially see in Figure 2.2: it is this complexity that makes it hard to concretely define and agree upon a single explanation and that prevents the establishment of effective treatments [5]. It also makes clear that when studying a specific path, one must remember the influence that parallel mechanisms can have in the experiment.

Bone is maintained by a continuous remodelling. The bone cells involved in bone remodelling are osteoclasts, osteoblast and osteocytes. Osteoblasts and osteoclasts form the basic multicellular unit and work coordinated in the process, being always in contact with the bone marrow, the origin of their precursors. Osteoclasts are large multinucleated cells that are originated from

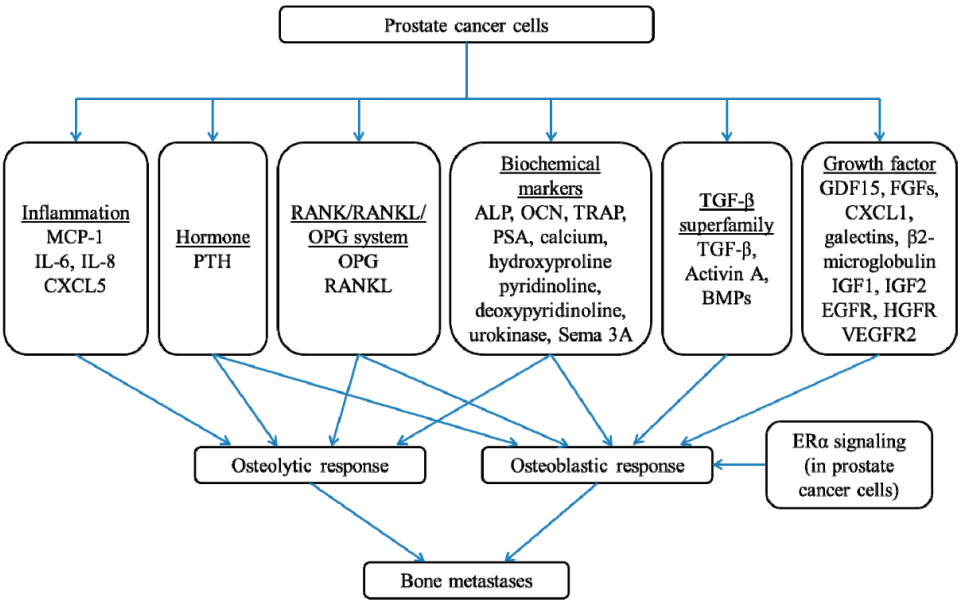

Figure 2.2: Schematic representation of how different paths contribute to the formation of PCa bone metastases [5].

macrophages and monocytes and secrete acid and collagenase. Osteoblasts are single nucleated cells, differentiated from mesenchymal stem cells, that have the capacity of producing bone ECM.

Bone remodelling is a complex process that starts with bone resorption by osteoclasts. This bone resorption is normally balanced by bone formation by the osteoblasts. Lastly, the osteocytes are formed, derived from osteoblasts that become surrounded by ECM, ending up embedded in the mineralized bone matrix. Their function is maintaining the bone tissue [4, 26–28].

Globally, when cancers form bone metastases, they are primarily osteolytic, characterized by bone dissolving. However, PCa bone metastases are mostly osteoblastic, leading to the formation of new bone. In fact, PCa cells demonstrated an osteoblastic-like phenotype, in some reports [27]. Nevertheless, even in osteoblastic cancers, there is a significantly accelerated bone resorption and this phenomenon is responsible for the growth factors release, promoting tumour growth [26] Also, this simultaneous presence of osteoblastic and osteolytic lesions, from a clinical point of view, complicates the establishment of a bone-specific therapy [5].

The source of the bone-forming cells recruited for PCa bone metastases is poorly understood. In the beginning, it was only attributed to osteoblast precursors present in the bone marrow or in the circulation, activated and recruited by the imbalance in the bone-forming process caused by the cancer cells presence. Recently, the origin of these cells is being partially credited to endothelial-to-osteoblast conversion. Endothelial cells have remarkable plasticity and can be converted into multiple cell types. Studies have shown that endothelial cells can be converted into osteoblasts by factors secreted by PCa cells, even passing by a phase of endothelial-osteoblast hybrid cells [27, 29].

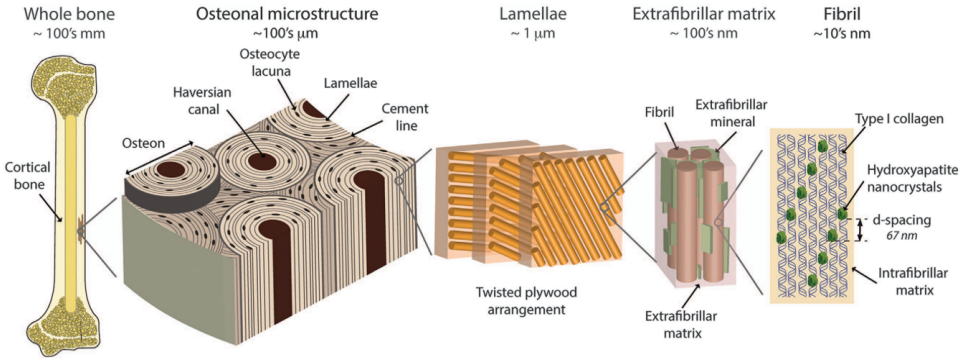

Figure 2.3: Hierarchical structure of human cortical bone. At the nanoscale the bone is composed of two elements: col-I and HA nanocrystals. At the microscale, it is possible to find lamellae and osteons. At the macroscale, the bone structure is divided into cortical bone (hard) and trabecular bone (spongy) [30].

2.2.1 Bone microenvironment

The bone microenvironment is a very complex system: it contains a biological component, composed by the haematopoietic and mesenchymal cell lines, the vasculature and the bone marrow stroma; and a structural one, the ECM, that makes up most of the dry weight of bone. Both these components play very important roles in bone metastases [26, 28].

The bone ECM can participate in the metastization process since [26]:

- it is very rich in growth factors, that are very important since they can control the phenotype of the tumour cells and, consequently, the aggressiveness of the metastatic lesions;
- its physical properties, structure and even local changes create a favourable environment for tumour growth;
- it contains several non-collagenous proteins, like SPARC, that can interact with the cancer cells;
- it also plays an important role in the differentiation process of mesenchymal stem cells into osteoblasts.

The bone microenvironment is organized in a hierarchical structure (Figure 2.3). At the most basic level, it is possible to find an array of col-I fibrils with nanocrystals of hydroxyapatite (HA) embedded. There are an intrafibrillar and an extrafibrillar matrix, containing non-collagenous proteins and enzymatic and non-enzymatic cross-links. These collagen fibrils assemble into lamellae, that form osteons, that make the microstructure of the cortical bone, that is a part of the macroscopic whole bone [30].

Thus, the ECM itself is organized into two components: a mineralized portion, HA nanocrystals (calcium-phosphate), and an organic portion, col-I (94%) and other non-collagenous proteins.

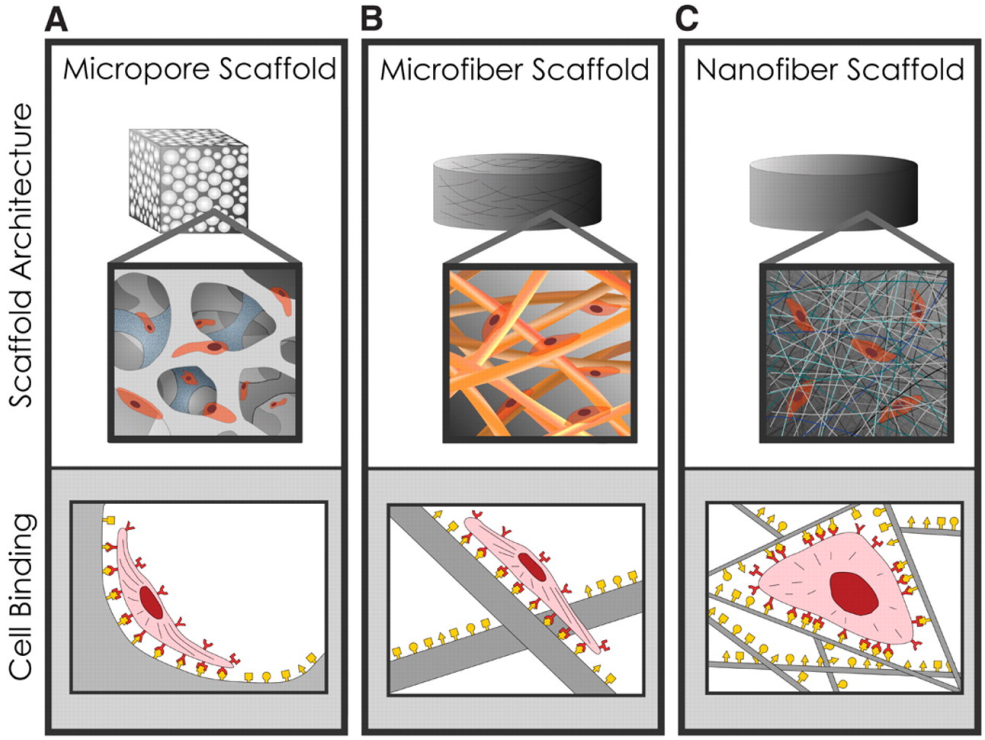

Figure 2.4: How the scaffold architecture affects cell binding and spreading. In the microscale (A and B) cells acquire a 2D flatten configuration. Only in the nanoscale (C) is possible to have the number necessary of binding sites to a cell acquire a more natural behaviour [32].

Bone, a mineralized connective tissue, receives its mechanic characteristics from its different components. The mineralized portion of the ECM gives bone its rigidness and hardness, while the organic part defines its flexibility, its elastic modulus, and its high ductility [28, 31].

2.2.2 Bone biomimetic biomaterials

The ECM is in the nanoscale and, as seen before, is very complex. Nowadays, engineered biomimetic materials become more and more similar to that level of complexity. This is very important because it has been proved that cells are intrinsically susceptible to their environment.

When comparing a 2D model with a 3D one, it is possible to observe differences between the binding of integrins, the formation of focal adhesions, the structure, localization and function of a tissue composed by cells growing in that scaffold. Logically, 3D configuration allows cells to obtain a more natural behaviour.

Scaffolds with nanoscale structures can be used to control cell behaviour and even the conformation of adsorbed proteins (Figure 2.4). Actually, even increasing the surface roughness of a scaffold pore has been proved to increase cell attachment, proliferation and expression of ECM components. The next step is combining scaffolds at the nanoscale with the use of naturally derived materials, such as biopolymers, and the addition of biological signals, such as growth factors and proteins. Naturally, this has some challenges attached to [32].

Scaffolds are designed to be a simplistic but faithful version of the microenvironment observed in real organs. Considering all that has been said before about the bone microenvironment, an obvious scaffold for bone applications would consist in a col-I nanofibres matrix with a HA nanocrystals disperse phase, this is, a biocomposite. To manufacture at the nanoscale, several techniques have been used and between them, it is possible to find electrospinning and electrospraying.

2.2.3 A biocomposite of collagen nanofibers and nanohydroxyapatite

Electrospinning and electrospraying are processes where, with a high voltage source, a high potential electric field is applied to the dispersion of a solution, allowing it to be spun or sprayed to obtain fibres or particles, respectively, at the nanoscale order. The setting difference between the techniques is the flow rate.

Electrospraying (from electrostatic spraying), as stated before, involves the production of highly charged droplets. These droplets are self-dispersing, preventing agglomeration. Upon evaporation, they leave behind solid particles, so, electrospraying may be used as a micro and nanoparticle production technique. The droplets and the particles they origin have a low standard deviation in terms of diameter. Electrospraying is a low cost and very versatile technique, that counts with many applications in the literature [33, 34].

Electrospinning (from electrostatic spinning) may be considered a variant of electrospraying. Electrospinning allows the formation of fibres by the elongation of a jet of a viscoelastic polymer solution due to electrostatic repulsions and evaporation of the solvent. The thinner the fibres obtained are, the lower the solution flow rate must be, so the solvent has enough time for evaporation. Therefore, electrospinning is a slow technique. Other factors, such as the concentration of the solution, contribute to the diameter of the fibres. Li and Xia [35] stated that developing fibres with diameters in the 10 nm to 30 nm was not an easy task. ECM col-I fibres have diameters between 20 nm and 40 μm [12].

One common problem with electrospun fibres is the presence of beads and it can be due to many factors, such as the distance between the tip of the syringe with the solution and the collector, and the room humidity levels. Nevertheless, electrospinning may be a good solution to mimic ECM and it is a simple, inexpensive and versatile technique [35, 36].

As said in Chapter 1, the work of Ribeiro *et al.* [12] will be followed for the fabrication of the biomaterial: a biocomposite of electrospun col-I nanofibres and electrosprayed nanophased HA (nanoHA) crystals. In this report, the experimental setting used allows simultaneous electrospraying and electrospinning (Figure 2.5), by a patented technique [37], and the protocol leads to the formation of col-I fibres with a mean of 30 nm of diameter, in the same size parameters of natural col-I fibres in bone ECM.

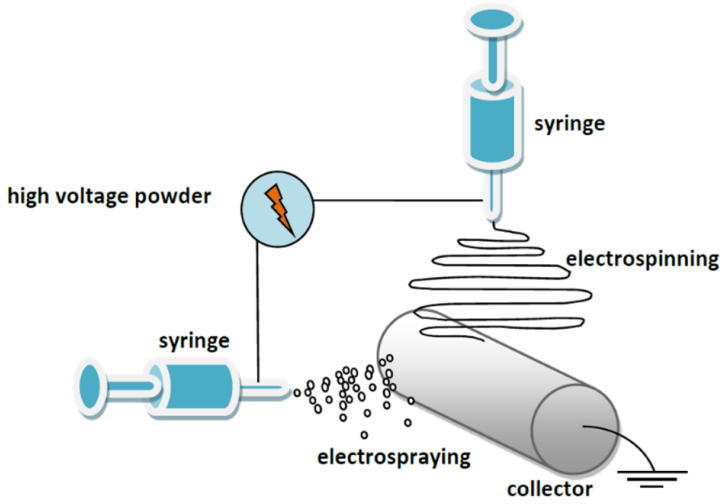

Figure 2.5: Schematic of the experimental setting used for simultaneous electrospraying and electrospinning [37].

2.3 Prostate cancer, endothelial and osteoblasts cell lines

LNCaP and PC-3 are among the most commonly used human PCa cell lines for research proposes. Lymph Node Carcinoma of the Prostate (LNCaP) is a cell line obtained from PCa lymphatic metastases, androgen-sensitive [‡] and that expresses PSA. LNCaP is highly aneuploid and has a doubling time of about 60 hours. PC-3 is a cell line derived from PCa bone metastases in vertebrae, androgen-resistive and that does not express PSA. PC-3 cells have a doubling time of about 33 hours and are 100% aneuploid [38].

It has been shown that PC-3 has a preference for adhering to bone marrow-derived mesenchymal stem cells (osteoblast progenitors) and higher affinity to col-I than LNCaP. Also, PC-3 has col-I binding integrin receptors. These findings can explain how PC-3 has a higher tendency to spread to the bone then LNCaP [39]. Both LNCaP and PC-3 express alpha-methylacyl-CoA racemase (AMACR), a PCa mitochondria and peroxidase biomarker, however, it has been proved that the expression is stronger for LNCaP since AMACR is less expressed by poorly differentiated cell lines [40].

Endothelial cells form the vascular endothelium and have as functions the oxygen and nutrients delivery throughout the body, the vessel integrity maintenance and patrolling immune cell trafficking. They play a crucial role in the regulation and coordination of angiogenesis [41]. For setting up experimental models to study mechanisms like angiogenesis, tumour growth and metastasis, human microvascular endothelial cells are regularly used. Human Pulmonary Microvascular

[‡]Androgen deprivation therapy is a hormone therapy where the levels of male hormones, androgens, are reduced in an attempt to minimized PCa growth. This way, the different types of PCa can be classified as androgen-sensitive (or castrate-sensitive) and androgen-resistive (or castrate-resistant), depending on if they are sensitive or resistive to androgen deprivation therapy [3].

Endothelial Cells ST1.6R (HPMEC-ST1.6R) is an endothelial cell line that has a broad spectrum of endothelial phenotypic markers, hence the use of this cell line in *in vitro* model systems. One of the phenotypic markers is the expression of the cluster of differentiation 31 (CD31), an endothelial cytoskeleton biomarker [42].

2.4 Secreted protein, acidic and rich in cysteine (SPARC)

SPARC is a secreted matricellular glycoprotein that does not serve a primarily structural role but instead mediates cell-matrix interactions, being a member of the follistatin-related protein family. When it was originally identified, as osteonectin, it was described as a bone-specific phosphoprotein that binds selectively to collagen fibrils and HA [43] and, in fact, SPARC is a major bone matrix non-collagenous protein that binds to calcium. However, SPARC is secreted by different cell types, such as osteoblasts, fibroblasts, endothelial cells and platelets.

In vitro and *in vivo* experiments have allowed to attribute to SPARC several functions, regarding multiple biological processes. Between them, SPARC:

- modulates cell proliferation, through inhibition of binding to cell-surface receptors;
- modulates cell spreading and attachment, promoting counteradhesion, by interacting with ECM components such as collagen;
- is involved in bone mineralisation, binding strongly to col-I and HA;
- regulates matrix remodelling by influencing the metalloproteinases production;
- exhibit increased levels in remodelling tissues and during angiogenesis;
- promotes osteoblastogenesis;
- inhibits cell cycle progression from G1 to S phase in primary cells;
- reduces proliferation and migration of endothelial cells by regulating the activity of growth factors;
- regulates endothelial cell shape and barrier function and induces endothelial cell apoptosis;
- has a role in wound healing, increased expression in atherosclerotic tissue and inhibits adipogenesis. It may affect key functions in the adipose tissue;
- high levels of SPARC expression correlate with tumour progression for some types of cancer but, for others, SPARC has antitumor effects.

To sum it up, SPARC has been reported to promote cell proliferation, mineralisation, remodelling, angiogenesis, osteoblastogenesis but also to inhibit adhesion, differentiation, proliferation and migration of endothelial cells and adipogenesis [11, 44–46].

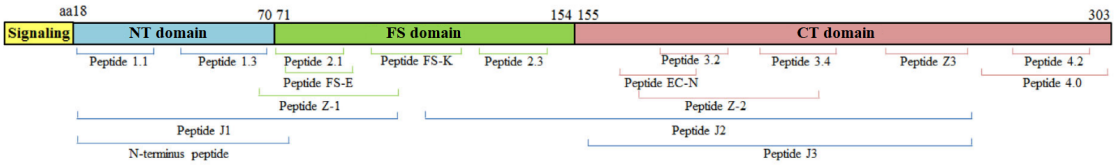

Figure 2.6: SPARC domains and peptides. Adapted from [11].

2.4.1 SPARC structure and peptides

The mature human SPARC consists of 286 amino acids (aa): it starts with 32,5 kDalton and 303 aa, but the first 17 aa contain a signalling peptide sequence that is removed during processing. The mature SPARC is divided into three distinct domains: an NH_2-terminal (NT) domain, a follistatin-like (FS) domain and a COOH-terminal (CT) domain.

The NT domain comprises 52 aa, is acidic, unstructured and mediates the interaction with HA. This domain contains immune dominant epitopes and, being rich in asparagine and glutamate, can bind 5-8 calcium ions with low affinity. This is the region that most separate SPARC from other genes of the same family.

The FS domain has 85 aa, is rich in cysteine, folds into an elongated nonglobular structure and contains several bioactive peptides. It connects the other two domains, stabilising the connection by a complex network of internal disulphide bonds.

The CT domain is 149 aa long, extracellular calcium-binding, globular and almost entirely α-helical. This domain contains two EF-hand motifs that bind Ca^{2+} with high affinity and also collagen type I, III V and IV bind to this domain, depending on it [11, 45, 46].

Inside these 3 domains, SPARC is divided into several peptides with different biological functions, as we can see in Figure 2.6. Among the peptides, it is possible to find SPARC 2.1 peptide, that inhibits the proliferation of endothelial cells, FS-E peptide, that potently inhibits endothelial cell migration *in vitro* and angiogenesis *in vivo*, 2.3 peptide, that has a stimulatory effect on endothelial cell proliferation and angiogenesis and also high affinity for Ca^{2+}, and 4.2 peptide, which stimulates endothelial cells migration but inhibits their proliferation and also binds to collagen and Ca^{2+} [11, 46].

2.4.2 SPARC and bone remodelling

SPARC is one of the most abundant non-collagenous protein found in the ECM of bone. SPARC contains both a collagen-binding and an HA-binding region so it has been proposed that SPARC binds to collagen and HA, releases calcium and enhances mineralisation of the collagen matrix in bones. These binding regions are in the CT and the NT domains, this is, in opposite sites of SPARC, and this separation has been proposed to facilitate the mineralisation process. However, attachment to collagen has been simultaneously reported to promote and to inhibit HA formation. High levels of SPARC have been recorded in osseous tissue with high turnover and mineralisation, whereas mature bone reported low levels of the protein [11, 31].

Osteopenia is characterised by a decrease in bone mineral density and is considered a precursor to osteoporosis. Experiments with SPARC-null mice show decreased numbers of osteoblasts and osteoclasts which indicates decreased bone remodelling, leading to profound osteopenia. There was a decrease in the volume of trabecular bone, but not in cortical bone, which is consistent with the fact that trabecular bone has 20-to-40-fold more SPARC than cortical bone. However, both trabecular and cortical bone showed decreased matrix content and less bone stiffness [47]. Later, other studies indicated that osteoblastic precursors were reduced and osteoblast differentiation was impaired [31].

Increased levels of SPARC expression correlate with mature collagen accumulation and fibril assembly into the ECM of many connective tissues. The presence of SPARC also has been reported to allow thick collagen fibres organised into longitudinal bundles [11, 31].

The mechanisms by which SPARC influence bone formation and maintenance may include regulation of procollagen processing, by modulating integrin engagement, and also collagen assembly in the ECM, crosslinking and mineralisation. SPARC also may control osteoclast and osteoblast differentiation and activity. In summary, SPARC plays a critical role in regulating bone remodelling and maintaining bone mass and mechanical properties, being essential for proper ECM assembly and architecture [11, 31].

2.4.3 SPARC and cancer

As early mentioned, it is known that SPARC has a role in cancer, however, for each type of cancer, it seems to have different behaviours. The type of cells that express the protein, the malignant cells or the neighbouring stromal cells, also influences the expression. Some types of cancer even have contradictory reports, depending on the model studied. This makes SPARC involvement highly contextual and influenced by the microenvironment [11, 46].

It has been possible to relate SPARC with EMT. For example, several studies have stated that SPARC promotes EMT in melanoma cells, as it influences the cadherin switch and the expression of *VIM* and *SNAIL*. SPARC might also promote EMT induction by inducing collagen expression [11].

Concerning breast cancer, high SPARC expression levels are negatively associated with patients overall survival. However, there are some reports that oppose this affirmation, relative to tumours that show *BRCA1* mutation. Concerning the developing of therapy, some reports show that SPARC inhibits cancer proliferation, others report the opposite, depending on the model used [46]. More recently, Zhao *et al.* [48] and He *et al.* [49] propose the sintering of mesoporous selenium and transferrin-inspired/ferric ion nanoparticles (respectively) for drug release, interacting with the breast cancer cells SPARC, ensuring tumour-targeting and endocytosis of the nanoparticles.

Concerning melanoma, high SPARC levels are suggested as a biomarker for cancer, but there is not a consensus. In human samples, it seems that there are studies defending opposite views and even proving that SPARC is not a biomarker for the presence of cancer. However, in these last ones, tumours with high expression of SPARC seem to correlate with metastatic disease. Studies have shown that the suppression of SPARC expression leads to inhibition of tumour growth.

In brain tumours, in general, the overexpression of SPARC seems to correlate with tumour invasiveness. However, it depends on the type of tumour. In gliomas, more aggressive tumours but that rarely metastasise, SPARC seems to induce EMT and promote cell survival and invasion. In neuroblastomas, most common, SPARC seems to function as an anti-angiogenic factor, inducing apoptosis of the endothelial cells.

Regarding ovarian cancer, in several studies, SPARC seems to induce apoptosis of the cancer cells. The absence of SPARC resulted in high expression of growth factors, hence angiogenesis and metastization. However, different studies seem to give a different conclusion regarding if the upregulation of SPARC has a negative or positive effect in human ovarian cancer, but this may be attributed to the SPARC antibodies used.

In colorectal cancer, SARC expression seems to be upregulated in the stromal cells, but not in the epithelium of the tumour. There was a positive correlation between SPARC and the clinical outcome. The presence of SPARC seemed to enhance the effectiveness of chemotherapy [11, 46].

The differential expression of SPARC by different tumours does not consist of an obstacle to its use in cancer therapy. In low SPARC expressing tumours, administration of SPARC or SPARC peptides may conduce to tumour regression. In high SPARC expressing tumours, SPARC may be used as a biomarker and as a mean of mediating the administration of drugs [46].

2.4.4 SPARC and PCa

Regarding PCa, metastatic cells display higher levels of SPARC than non-metastatic and normal prostate. However, when considering tumour aggressiveness, SPARC expression is decreased in the most aggressive metastatic tumours, which leads one to conclude that SPARC may function as a tumour biomarker but also as a tumour suppressor.

High SPARC expression levels are also associated with PCa bone metastasis. Indeed, SPARC seems to be a key part of the attraction of PCa to bone. However, *in vivo* experiments with SPARC-deficient mice revealed that bone stromal SPARC inhibited PCa expansion. [11, 46].

Nevertheless, SPARC in PCa also presents some inconsistencies regarding the results of several studies. In Table A.1 (Appendix A), the most relevant studies regarding SPARC and PCa, of the last 3 years (2016-2018) are presented, stating the models used and the main conclusions.

Of these studies, most were consistent regarding the high SPARC expression in PCa cells, when compared to normal prostate. SPARC was tested as a bone-metastatic and PCa biomarker, chosen as a target for gene therapy, its inhibition by microRNAs and gene hypermethylation was accessed and proteins of the same family were studied. Most of the studies included the analysis of histological samples from several patients, a few resorted to *in vivo* models with nude mice and some presented *in vitro* models results. However, only two studies, Ribeiro *et al.* [50] and Cruz-Neves *et al.* [51] presented an *in vitro* model based in a biomimetic biomaterial and this was the one described in Ribeiro *et al.* [12].

In Ribeiro *et al.* [50], bone metastatic PCa cells, PC-3, presented 8-fold SPARC expression than non-bone metastatic PCa cells LNCaP. The biomaterial seemed to induce the expression of SPARC in LNCaP cells. In Cruz-Neves *et al.* [51], these results were confirmed and LNCaP

seemed to only be able to proliferate passed 21 days in a bone-like environment in the presence of SPARC.

Chapter 3

Materials and Methods

3.1 Manufacturing the biocomposite

The biocomposite was produced according to the protocol optimised by Ribeiro *et al.* [12].

3.1.1 Electrospinning and electrospraying

A 12% (w/v) collagen solution was prepared by dissolving bovine col-I (Kensey Nash Corporation) in a solution of acetic acid glacial:ethyl acetate:water (40:30:30) and letting it stir overnight at 4 ^{o}C. The solution was prepared and loaded into a syringe with a 21 G needle.

Simultaneously, a 3.5% (v/v) nanoHA solution was prepared by dissolving HA aqueous paste 15% wt. (Fludinova S.A.) in methanol. The solution was subjected to 20 minutes of stirring, submitted to two cycles of 10×15 ultrasonic pulses (amplitude 60 A) to decrease the nanocrystals agglomeration and loaded into a 21 G needle syringe.

Once prepared, the col-I solution was electrospun at 0.1 mL/h and the nanoHA solution was electrosprayed at 2 mL/h, concurrently, to the same rotating cylinder collector, at 400 rpm (Figure 3.1). Both needles were placed at a 12 cm distance from the collector and a 20-kV voltage was applied. As physical support for the biomaterial, 10 or 15 mm of diameter cover glasses were used, attached to an aluminium foil wrapped in the cylinder collector.

These processes were performed for 1 hour per aluminium foil at room temperature (27.3 ^{o}C to 30.6 ^{o}C) with a relative humidity of 36.0% to 42.8%.

3.1.2 Substrate characterization

The integrity and 3D structure of the biomaterial were examined recurring to scanning electron microscopy (SEM). SEM analysis was performed using an FEI Quanta 400FEG/EDAX Genesis X4M (FEI Company) scanning electron microscope, under high vacuum conditions. To allow the analysis, the samples were sputtercoated with a thin palladium–gold film. The diameter of representative random fibres was analysed and compared to the literature.

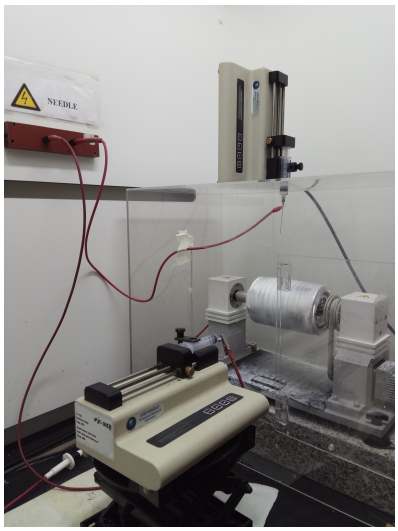

(a)

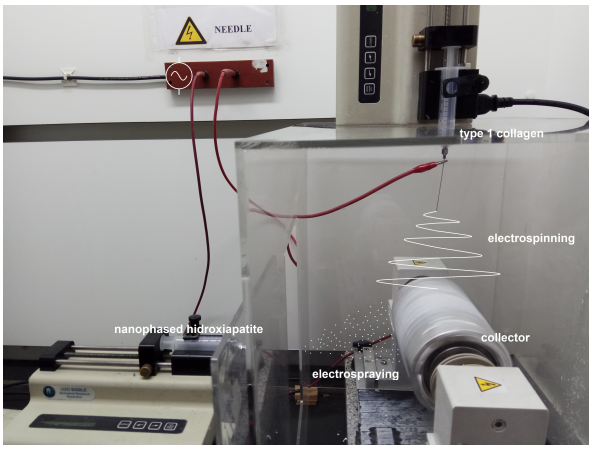

(b)

Figure 3.1: Experimental setting used for simultaneous nanoHA electrospraying and col-I electrospinning. (a) A general view. (b) A closed-up view with a scheme.

3.1.3 Cross-linking and disinfection

To provide mechanical strength to the fibres, a cross-linking protocol was implemented. To do so, the samples were in contact with a 90% (v/v) ethanol solution containing 20 mM N-(3-dimethylaminopropyl)-N-ethylcarbodiimide hydrochloride (Fluka) and 10 mM N-hydroxysuccinimide (Fluka), overnight at 4^{o}C. After cross-linking, the material was washed 3 times with 90% (v/v) ethanol solution and 2 times with pure water and left to dry overnight at room temperature in a desiccator.

In the flow chamber, the biomaterial was submerged for 10 minutes in decreasing concentrations, 90%, 70% and 50% (v/v), of filtered ethanol solutions and then washed with filtered pure water, before cell seeding.

3.2 Cell culture

Cell cultures were conducted in the biomaterial, functionalized with SPARC and SPARC peptides. Monocultures of PC-3, LNCaP and HPMEC-ST1.6R and co-cultures of PC-3/HPMEC-ST1.6R and LNCaP/HPMEC-ST1.6R were conducted for assessing cell metabolic activity, proliferation and morphology and gene expression.

All chosen cellular seeding densities and times of culture are optimized values of previous experiences.

3.2.1 PCa and endothelial cell lines

LNCaP and PC-3 cells were maintained in RPMI medium (Gibco) and RPMI/F12 medium (Gibco), respectively, both supplemented with 10% (v/v) foetal bovine serum, FBS, (Sigma-Aldrich) and 1% (v/v) of penicillin-streptomycin (Gibco).

HPMEC-ST1.6R cells were grown in M199 medium (Sigma-Aldrich) with 20% (v/v) FBS, 1% (v/v) of penicillin-streptomycin, 1% (v/v) of glutamax-I (Gibco), 1:1000 geneticin (Gibco) and 1:1000 endothelial cell growth supplement/sodium heparin (Enzifarma), in plastic culture flasks coated with 0.2% (w/v) gelatine from porcine skin (Sigma-Aldrich).

All cell lines were cultivated in 25 cm^2 plastic culture flasks, incubated in a humidified chamber at 37 ^oC and 5% CO_2 and routinely tested for mycoplasma contamination through PCR.

3.2.2 Cell seeding

In total, six different conditions were tested for cell seeding:

- seeding in cover glasses coated with poly-D-lysine (PDL);
- seeding in biomaterial;
- seeding in biomaterial with pre-adsorbed SPARC with a concentration of 0.23 μM (10 μg/mL);
- seeding in biomaterial with pre-adsorbed SPARC with a concentration of 0.69 μM (30 μg/mL);
- seeding in biomaterial with pre-adsorbed SPARC 2.3 peptide with a concentration of 23 μM (46.2 μg/mL);
- seeding in biomaterial with pre-adsorbed SPARC 4.2 peptide.

PDL coated cover glasses were used for control purposes. The coating was applied to cover glasses stored in a 70% (v/v) ethanol solution (for at least 30 minutes) and washed with pure water. PDL (Sigma-Aldrich) 0.1 mg/L solution was applied for 30 minutes at room temperature and washed again with water.

All the substrates were placed in 24-well plates. When it was the case, biomaterial samples were adsorbed with SPARC (Sigma-Aldrich) and SPARC peptides, for an hour, at room temperature, and washed carefully with phosphate buffered saline (PBS) solution.

Peptide 4.2 was purified from a bis-thiol precursor with a final purity degree of 95.8%. Peptide 2.3 was synthesized and purified with a final purity degree of more than 99.9%.

3.2.2.1 Monocultures

HPMEC-ST1.6R, LNCaP and PC-3 were cultured with a single seeding density of 4×10^4 cells/mL in their correspondent culture medium.

Confluent cultures were rinsed with PBS solution, detached with 0.5% (w/v) trypsin for 5 minutes at the humidified chamber and resuspended again in the correspondent culture medium. Cells were counted with a Neubauer chamber and seed with the chosen seeding density in the biomaterial and control samples. The 24-well plates were incubated in a humidified chamber at 37 ^{o}C and 5% CO_2 for 5 days, being the incubation medium changed once.

3.2.2.2 Endothelial/PCa cells co-cultures

Before peptide adsorption, the biomaterial samples were incubated for 30 minutes in HPMEC-ST1.6R complete medium.

HPMEC-ST1.6R was cultured first with a seeding density of 1×10^4 cells/mL, in a procedure similar to the one described for monocultures.

The incubation medium was a mix of 50% (v/v) HPMEC-ST1.6R complete medium and 50% (v/v) of PCa complete medium, corresponding to previously optimized percentages that allowed cell growth and adhesion to the biocomposite. The 24-well plates were incubated in a humidified chamber at 37 ^{o}C and 5% CO_2 for 4 days.

At the end of the 4 th day, PCa cells were seeded on top of the endothelial cells, starting the co-cultures. LNCaP or PC-3 were cultured with a seeding density of 4×10^4 cells/mL. The co-cultures were incubated for 5 days in the same conditions, being the incubation medium changed once.

3.2.3 Metabolic assay

Cell metabolic activity was evaluated with resazurin assay. In this assay, viable cells can be distinguished from dead cells by a fluorescence signal generated by the reduction of resazurin (blue and non-fluorescent) into resorufin (pink and highly fluorescent) (Figure 3.2) [52].

Samples without cells were incubated with complete medium, to serve as blank. At the end of 1, 3 and 5 days of incubation, 50 μL of a 10% (v/v) stock resazurin solution was added to each well and incubated for 3 hours at 37 ^{o}C and 5% CO_2, protected from the light. 100 μL of supernatant were transferred into a black 96-well plate to analyze the fluorescence, in a Synergy Mx microplate reader (BioTek), using wavelengths of 530 nm excitation and 590 nm emission.

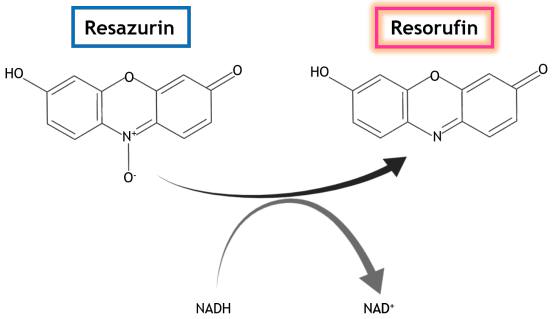

Figure 3.2: Substrate and products of the resazurin reduction reaction. Created with www.BioRender.com

After performing each assay, the samples were washed with PBS solution, the complete medium was replaced and the incubation continued, being the samples discarded at the end of the last assay.

The mean fluorescence value corresponding to the blanks was subtracted to each measure and the results were presented in reference fluorescence units (RFU) per cm^2, corresponding to the mean $\pm$ standard deviation of six samples.

3.2.4 Cell fixation

Before accessing cell proliferation and morphology, monocultures and co-cultures were conducted and fixed with paraformaldehyde. At the end of either 1, 3 or 5 days of incubation, the incubation medium was discarded and the samples were washed twice with PBS solution and fixed in 200 μL of 4% (v/v) paraformaldehyde (Sigma-Aldrich), for 15 minutes, at room temperature. After washing again twice, the 24-well plates were kept in PBS solution at 4 ^{o}C.

3.2.5 4.2 peptide

The tested SPARC and 2.3 peptide concentrations were chosen based on the previous work results. For choosing a 4.2 peptide concentration, four concentrations were absorbed in biomaterial, for one hour: 0.0023 μM (0.00517 μg/mL), 0.23 μM (0.517 μg/mL), 23 μM (51.7 μg/mL) and 230 μM (517 μg/mL). Samples without peptide were used as control. HPMEC-ST1.6R was seeded on these samples and cultured for 5 days. Resazurin assays were performed at the end of 1, 3 and 5 days of incubation.

3.2.6 Pellet obtention

Monocultures and co-cultures were conducted for obtaining pellet to evaluate gene expression. At the end of the 5 th day of incubation, cells were detached with trypsin by the previously referred method. Every 3 wells of the same condition were collected to a tube and centrifuged for 5 minutes

at 1200 rpm. The supernatant was rejected; the pellet was washed with PBS solution and again centrifuged for 5 minutes at 2000 rpm. The obtained samples were kept at -80 ^{o}C.

3.3 Gene expression

Samples obtained in cell culture were used for assessing gene expression related to EMT and angiogenesis, by performing real-time reverse transcription polymerase chain reaction (RT-PCR).

Real-time PCR allows the detection and quantification of the product accumulation as the amplification reaction progresses in time, by allying regular PCR methods to spectrophotometry. For that propose, fluorescent molecules whose fluorescence increases with the DNA amount are added to the reaction. As an advantage over conventional techniques, real-time PCR can give quantitative results, in which case it is called quantitative PCR (qPCR) [53].

3.3.1 RNA extraction

RNA extraction was performed by adding 500 μL of TripleXtractor (GRiSP) to each pellet obtained, homogenising with a syringe and letting it incubate for 5 minutes, at room temperature. The samples were transferred to an RNase free centrifugation tube with 100 μL of chloroform (Merck), vortexed and incubated, for 3 minutes at room temperature.

The samples were centrifugated for 15 minutes, at 4 ^{o}C, at 13 000 rpm, and the supernatant was transferred again to an RNase free centrifugation tube. 250 μL of isopropanol was added and, after vortex, it was incubated for 10 minutes at room temperature to allow RNA precipitation.

A second centrifugation was performed for 10 minutes, at the same temperature and speed. This time, the supernatant was discharged, and the pellet was washed twice with 500 μL of 75% (v/v) ethanol solution, vortex and centrifugation for 5 minutes (same conditions).

The pellets were dried at air and, once dry, were resuspended in 20 μL of RNA Storage Solution and kept in ice for at least 30 minutes, being stored at -80 ^{o}C.

3.3.2 Reverse transcription

Complementary DNA (cDNA) was obtained from the extracted RNA by reverse transcription (RT). Before the cDNA synthesis, RNA quantification was performed for all samples, using a NanoDrop Lite spectrophotometer (Thermo Fisher Scientific). This way, samples were screened for low quantity of RNA as well for contamination with proteins.

250 to 1000 ng/mL of RNA of each sample were converted to cDNA using a RevertAid RT Reverse Transcription Kit (Thermo Fisher Scientific) and a Thermal Cycler (Bio-Rad). First, the already diluted samples were incubated with random hexamer primer, at 65 ^{o}C for 5 minutes. Then, a mix of X reaction buffer, 20 U/μL RiboLock RNase Inhibitor (Thermo Fisher Scientific), 10 nM dNTP mix and 200 U/μL RevertAid RT was added to each tube. After a gentle mix and brief centrifugation, the samples were incubated for 5 minutes at 25 ^{o}C, followed by 60 minutes at 42 ^{o}C and 5 minutes at 70 ^{o}C. The RT product obtained was stored at -20 ^{o}C.

3.3.3 Real-time PCR

cDNA was used to performed real-time PCR to access gene expression. The protocol was implemented for *CDH2*, *CDH1*, *TWIST*, *ZEB1*, *VIM*, *SNAIL*, *DDR1* and *SPARC* genes and β-glucuronidase (β-*GUS*) was used as a housekeeping gene, since its low expression variability has been proved among cancer cells [54, 55].

NZYSpeedy qPCR Green Master Mix (NZYTech, Lda.) with 0.4% (v/v) ROX was used. To 5 μL of the mix, 0.5 μL of primers (reverse and forward mix) were added. The final mix was added to 4.5 μL of the sample, performing a 10 μL final volume for analysis, in a sealed 384 plate.

After centrifugation, real-time PCR was performed in a LightCycler 480 System (Roche): 2 minutes at 95 ^{o}C followed by 40 cycles of 5 seconds at 95 ^{o}C and 30 seconds at the temperature of annealing optimised for the gene. The temperature of annealing and primers concentration per each tested gene was optimized and are expressed in Table 3.1.

Table 3.1: Optimized temperature of annealing and concentration under the final volume (10 μL) for each pair of primers used.

	Temperature of annealing ^{o}C	**Primers concentration** % (v/v)
β-GUS	60	5
CDH2	60	5
CDH1	64	5
DDR1	60	5
SNAIL	60	5
SPARC	60	5
TWIST	60	3
VIM	60	5
ZEB1	60	3

3.3.4 Data analysis

As previously mentioned, real-time PCR allows the detection in real-time of the DNA amplification through fluorescence. In the first PCR cycle, fluorescence levels are at background levels but, eventually, there is enough DNA amplified to lead to a detectable fluorescent signal. The threshold cycle (C_T) is the cycle number that corresponds to this detection threshold (Figure 3.3).

The C_T value can be related to the amount of template present at the beginning of the amplification: the smaller the C_T value, the higher the initial amount of template to amplify. Thus, in the optimization of the annealing conditions as mentioned above, the chosen parameters correspond to the ones that generate the lowest C_T values.

The most common methods implemented to analyse qPCR results are absolute quantification and relative quantification. The chosen analysis method was relative quantification normalized to a reference gene (also called housekeeping gene), in which the analysis results in a ratio. The

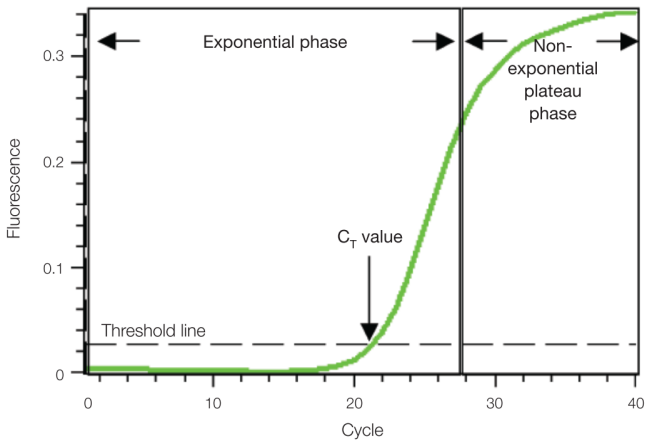

Figure 3.3: Real-time PCR amplification plot of relative fluorescence versus cycle number. Two phases can be identified, the exponential and the non-exponential plateau phase: since the C_T value is measured in the exponential phase, it can be used reliably to calculate the initial amount of DNA template [53].

samples cultured on biomaterial without peptide adsorption were used as a calibrator, being the expression of the target genes expressed in relative value to their expression.

The implemented method for relative quantification was the $2^{-\Delta\Delta C_T}$ method, also known as the Livak method. While it assumes an amplification efficiency near 100% for both target and reference genes and with a variation between them within 5%, it is a method widely used and easy to execute.

Three to four replicas were obtained for each condition tested and, for each one of these replicas, three measures were performed. The C_T value considered for the data analysis was the mean value of the three measures.

The first step to the Livak method, is to normalize the C_T value of the target gene to the value of the housekeeping gene, in this case, β-*GUS*, for all the conditions (equation 3.1):

$$\Delta C_T = C_{T(target)} - C_{T(\beta\text{-}GUS)} \tag{3.1}$$

Second, the ΔC_T of each test sample was normalized to the mean ΔC_T of the calibrator, in this case, the sample referred as biomaterial (equation 3.2):

$$\Delta\Delta C_T = C_{T(test)} - \bar{C}_{T(biomaterial)} \tag{3.2}$$

Lastly, the normalized expression ratio was obtained for each sample (equation 3.3), with the mean of the four replicas (upper and lower limit) as a result.

$$\text{Fold change} = 2^{-\Delta\Delta C_T} \tag{3.3}$$

Ultimately, the result obtained corresponds to the fold increase of the target gene in the test sample, relative to the sample cultured on the biomaterial without peptide and normalized to the expression of the β-*GUS*) gene [53, 56–58].

3.4 Cell proliferation and morphology

Immunostaining is a procedure in which specific antibodies, called primary antibodies, are used to detect one or more target protein. The antigen-antibody complex can then be signalized with immunofluorescence by recurring to a secondary antibody, directed against the invariant portion of the primary antibody and conjugated with a fluorophore [59]. Therefore, by choosing carefully the antibodies, it is possible to differentiate cell lines in a co-culture.

To access cell proliferation and morphology an immunostaining protocol was implemented, for the monocultures. Monoclonal CD31 and AMACR were chosen for primary antibodies, since they are known endothelial and PCa markers, respectively.

The results were analysed in an inverted fluorescence microscope (IFM), model AxioVert 200 M (Carl Zeiss Microscopy, LLC), and in a laser confocal scanning microscope (LCSM), model LCS SP2 AOBS (Leica Microsystems Heidelberg GmbH).

3.4.1 Immunostaining

After being washed with PBS solution, for 5 minutes, 3 times, the previously fixed samples were permeabilised with 150 μL of 0.2% (v/v) Triton X-114 in PBS solution, for 10 minutes, at room temperature. The samples were washed again 3 times, for 5 minutes, and incubated for an hour, at room temperature, in 150 μL of blocking buffer, 1.5% (w/v) bovine serum albumin (BSA) in PBS solution, to minimize non-specific adsorption of the antibodies.

The samples were then incubated with the primary antibodies, overnight, at 4 ^{o}C, protected from light. The primary antibody for HPMEC-ST1.6R cells was Monoclonal Mouse Anti-Human CD31 (Dako) and for PCa cells, it was chosen Rabbit Anti-Human AMACR (Leica), both diluted 1:100 in BSA in PBS solution.

After washing the samples (same way as before), they were incubated with the secondary antibodies for one hour, at 4 ^{o}C, in the dark. The secondary antibodies were Anti-Mouse Alexa Fluor 594 (Thermo Fisher Scientific), diluted 1:750 in blocking buffer, for HPMEC-ST1.6R cells and Anti-Rabbit Alexa Fluor 488 (Sigma-Aldrich), 1:500 in blocking buffer, for PCa cells.

After incubation and washing again, DAPI with VectaShield (Boster Biological Technology) was applied and the samples were kept in the dark, at 4 ^{o}C.

3.4.1.1 Protocol optimization

The protocol presented before was optimized by testing the concentration of the antibodies and the reagent of permeabilization. The concentrations tested for the antibody Monoclonal CD31 were 1:100 and 1:50, in blocking buffer. For the Triton X-114 in PBS solution, it was tested the application of a 0.2% (v/v) solution for 10 minutes and a 0.1% (v/v) solution for 5 minutes. The results were analysed in an IFM.

3.5 Statistical analysis

For the metabolic activity data, non-parametric one-way ANOVA followed by Bonferroni's multiple comparisons test, with a significance level of $p \leq 0.05$, was performed for each day individually, using GraphPad Prism version 6.01 (GraphPad Software). For the multiple comparisons test, the samples on biocomposite without peptide were used as control.

Regarding the gene expression data, since the $2^{-\Delta\Delta C_T}$ form may only be used for graphic representation of the data, a similar non-parametric analysis to the one above was performed on the corresponding ΔC_T values for each gene tested.

Chapter 4

Results

4.1 Collagen/nanoHA biocomposite

SEM analysis of the col-I/nanoHA biocomposite produced showed the structure described in the literature (Figure 4.1a). There were not visible a significant number of collagen beads (instead of fibres) or agglomerates of nanoHA with a considerable size.

It is important to notice that, in Ribeiro *et al.* [12], the biomaterial has been extensively characterized by other techniques, yet, SEM analysis is always mandatory because it allows conferring mesh integrity.

In Figure 4.1b it is possible to observe that the mean fibre diameter value is, in accordance with Ribeiro *et al.* [12], in the range of the natural bone ECM col-I fibres diameters: between 20 nm and 40 μm.

4.2 HPMEC-ST1.6R

Figure 4.2 shows the metabolic activity for the endothelial cell line, cultured on biomaterial with and without SPARC and 2.3 peptide adsorbed. Differences in the metabolic activity can only be spotted for the last day of growth, with both the SPARC and the peptide addition leading to a marked increase in endothelial cells proliferation.

Figure 4.3 shows the gene expression in HPMEC-ST1.6R, using the expression values for the cell culture in biomaterial as the reference.

Genes that were not expressed under any condition for one cell line were not included in the graphs: HPMEC-ST1.6R did not express *CDH1* and *TWIST* and it was not possible to find in the literature reports of the contrary.

It is possible to do two separate comparisons with the data: col-I/nanoHA biomaterial versus the chosen positive control (PDL) and col-I/nanoHA versus col-I/nanoHA with SPARC and SPARC peptides. These comparisons are summed up, for the 3 cell lines, in in Table B.1 and Table B.2, respectively, in Appendix B.

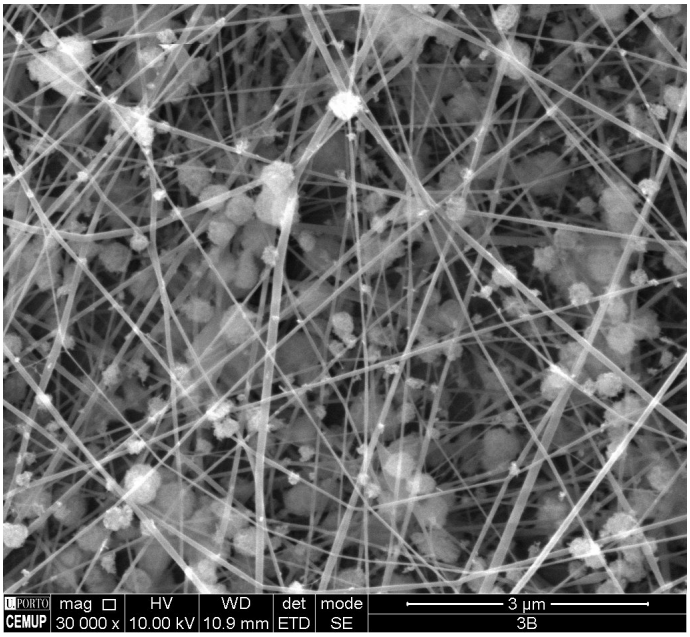

(a)

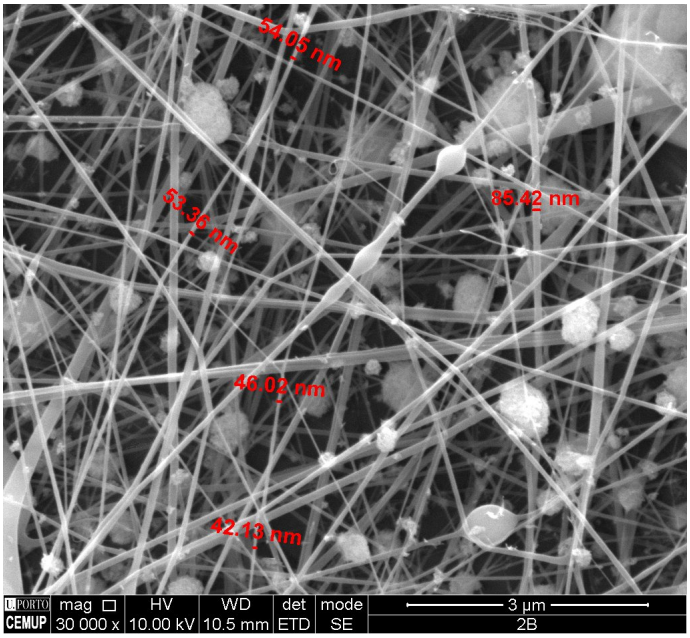

(b)

Figure 4.1: SEM images of the col-I/nanoHA biocomposite produced. Images obtained with a FEI Quanta 400FEG/EDAX Genesis X4M and opened with Fiji (ImageJ) software. 3 μm scale bar. (a) A representative capture. (b) 5 random fibres diameter measures.

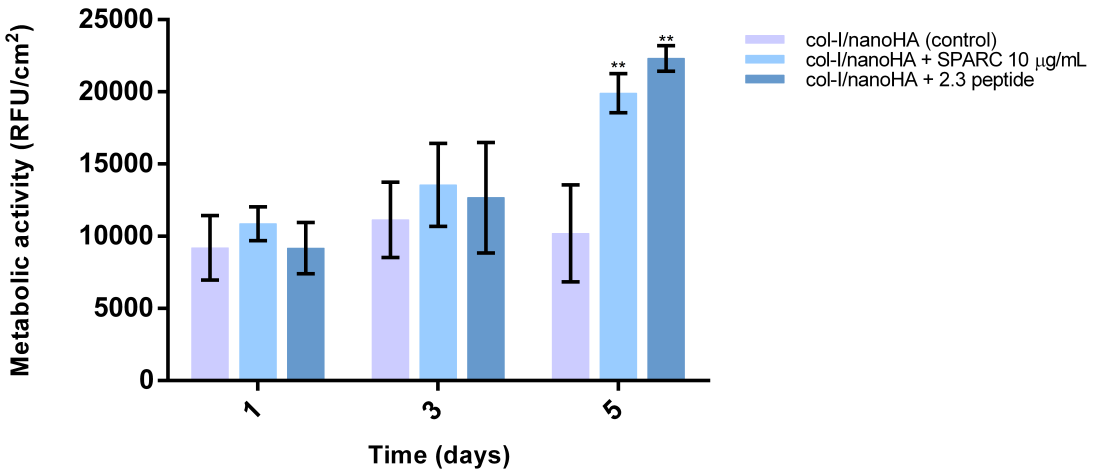

Figure 4.2: Metabolic activity in RFU per cm^2 for HPMEC-ST1.6R monocultures cultured on col-I/nanoHA biocomposite, functionalized with SPARC and SPARC 2.3 peptide, at the end of 1, 3 and 5 days of culture: col-I/nanoHA, col-I/nanoHA with SPARC 10 μg/mL and col-I/nanoHA with 2.3 peptide 46.2 μg/mL. Monocultures on biocomposite without peptide used as statistical standard. ** indicates statistical significance corresponding to $p \leq 0.01$. Results obtained with a Synergy Mx microplate reader. Graph and statistical analysis obtain with GraphPad Prism 6 software.

Concerning col-I/nanoHA biomaterial versus PDL, higher values were presented for expression in biomaterial for *CDH2*, *ZEB1*, *VIM*, *DDR1* and *SPARC*, some of them with a highly significant difference.

Concerning the SPARC and SPARC 2.3 peptide addition, significant decreases can be observed for almost all the expressed genes:

- *CDH2*: decreased expression in all conditions but with higher significance with SPARC 10 μL/mL and SPARC 2.3 peptide;
- *ZEB1*: decreased expression in all conditions but with higher significance with SPARC 2.3 peptide;
- *VIM*: decreased expression in all conditions but with higher significance in biomaterial with SPARC 10 μL/mL and 2.3 peptide;
- *SNAIL*: no statistical difference for all conditions;
- *DDR1*: it only showed decreased expression in biomaterial with SPARC 10 μL/mL;
- *SPARC*: showed significant decreases in all conditions but with higher significance in biomaterial with SPARC 30 μL/mL.

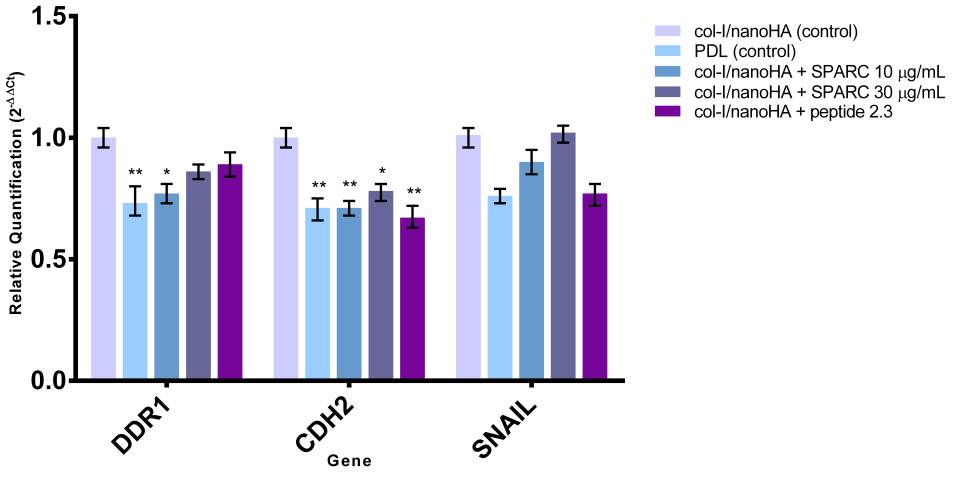

(a)

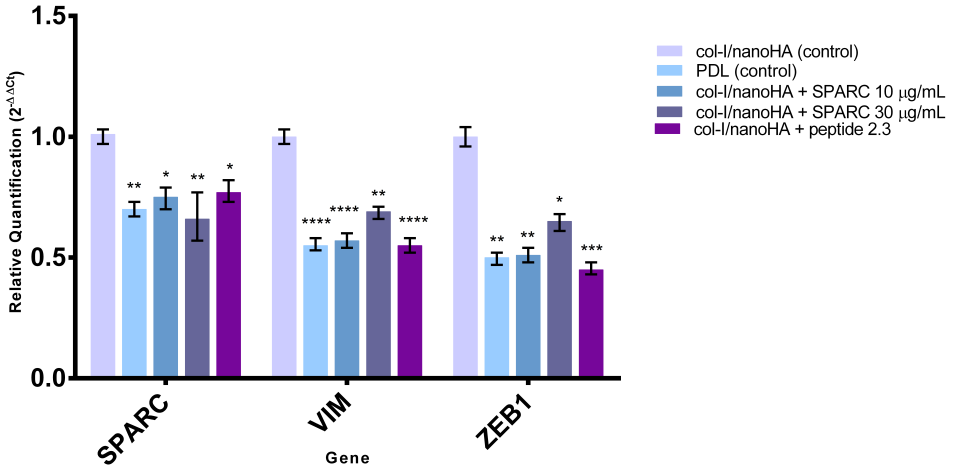

(b)

Figure 4.3: Gene expression in relative units for HPMEC-ST1.6R monocultures cultured on col-I/nanoHA biocomposite, functionalized with SPARC and SPARC 2.3 peptide, for 5 days: col-I/nanoHA, col-I/nanoHA with SPARC 10 μg/mL, col-I/nanoHA with SPARC 30 μg/mL and col-I/nanoHA with 2.3 peptide 46.2 μg/mL. Monocultures on PDL coated coverglasses were used as positive controls. Monocultures on biocomposite without peptide used as statistical standard. *, **, ***, **** indicate crescent levels of statistical significance, respectively, $p \leq 0.05$, $p \leq 0.01$, $p \leq 0.001$ and $p \leq 0.0001$. Graphs and statistical analysis obtained with GraphPad Prism 6 software. (a) *DDR1*, *CDH2* and *SNAIL* expression. (b) *SPARC*, *VIM* and *ZEB1* expression.

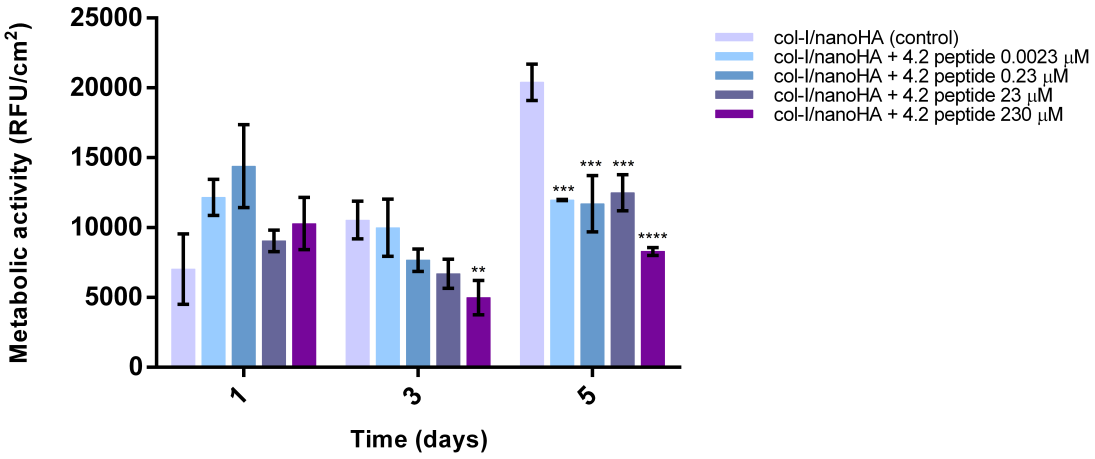

Figure 4.4: Metabolic activity in RFU per cm^2 for HPMEC-ST1.6R monocultures cultured on col-I/nanoHA biocomposite, functionalized with different concentrations of SPARC 4.2 peptide, at the end of 1, 3 and 5 days of culture: 0.0023 μM (0.00517 μg/mL), 0.23 μM (0.517 μg/mL), 23 μM (51.7 μg/mL) and 230 μM (517 μg/mL). Monocultures on biocomposite without peptide used as statistical standard. **, *** and **** indicate crescent levels of statistical significance, respectively, $p \leq 0.01$, $p \leq 0.001$ and $p \leq 0.0001$. Results obtained with a Synergy Mx microplate reader. Graph and statistical analysis obtain with GraphPad Prism 6 software.

4.2.1 HPMEC-ST1.6R and peptide 4.2

Figure 4.4 shows the metabolic activity assay results for 4.2 peptide concentration optimization.

A decrease of the endothelial cells metabolic activity was observed for all 4.2 peptide concentrations, at the end of 5 culture days. However, the most marked decrease is achieved for the 230 μM concentration. Since 4.2 peptide is associated with the inhibition of endothelial cells proliferation [11, 46], this concentration can be elected as the optimal concentration for the subsequent work.

4.3 LNCaP

Figure 4.5 shows the metabolic activity for the LNCaP cell line, cultured on biomaterial with and without SPARC and 2.3 peptide adsorbed. In the presence of exogenous 2.3 peptide, a cell proliferation increase can be identified on the third culture day, that latter disappears. For the SPARC addition, it seems to induce a decrease in cell metabolic activity, noticeable only in the last culture day.

Figure 4.6 shows the gene expression in LNCaP, using the expression values for the cell culture in biomaterial as the reference.

LNCaP did not express 3 genes and it was possible to find reports corroborating it: *CDH2* [60], *ZEB1* [61] and *TWIST* [62].

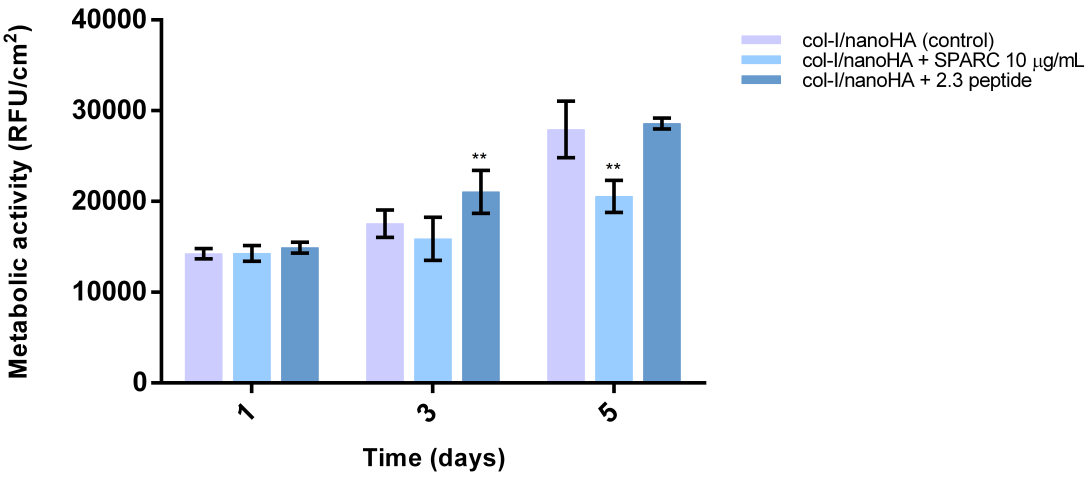

Figure 4.5: Metabolic activity in RFU per cm^2 for LNCaP monocultures cultured on col-I/nanoHA biocomposite, functionalized with SPARC and SPARC peptide, at the end of 1, 3 and 5 days of culture: col-I/nanoHA, col-I/nanoHA with SPARC 10 μg/mL and col-I/nanoHA with peptide 2.3 46.2 μg/mL. Monocultures on biocomposite without peptide used as statistical standard. ** indicates statistical significance corresponding to $p \leq 0.01$. Results obtained with a Synergy Mx microplate reader. Graph and statistical analysis obtain with GraphPad Prism 6 software.

Concerning col-I/nanoHA biomaterial versus PDL (Table B.1), LNCaP cells only presented a significant difference for the expression of *VIM*, being higher on biomaterial.

Concerning the SPARC and SPARC 2.3 peptide addition (Table B.2), LNCaP again only presented decreased expression for *VIM* with SPARC 10 μL/mL addition.

4.4 PC-3

Figure 4.7 shows the metabolic activity for the PCa cell line, cultured on biomaterial with and without SPARC and 2.3 peptide adsorbed. No statistical increases can be observed after the SPARC and SPARC peptide addition.

Figure 4.8 shows the gene expression in PC-3, using the expression values for the cell culture in biomaterial as the reference. All tested genes were expressed.

Concerning col-I/nanoHA biomaterial versus PDL (Table B.1), no significant difference was found for the expression of any gene.

Concerning the SPARC and SPARC 2.3 peptide addition (Table B.2), PC-3 cells only presented a statistical significant difference in expression in two situations: *CDH1* expression was increased with SPARC 30 μL/mL and *CDH2* expression was decreased with 2.3 peptide.

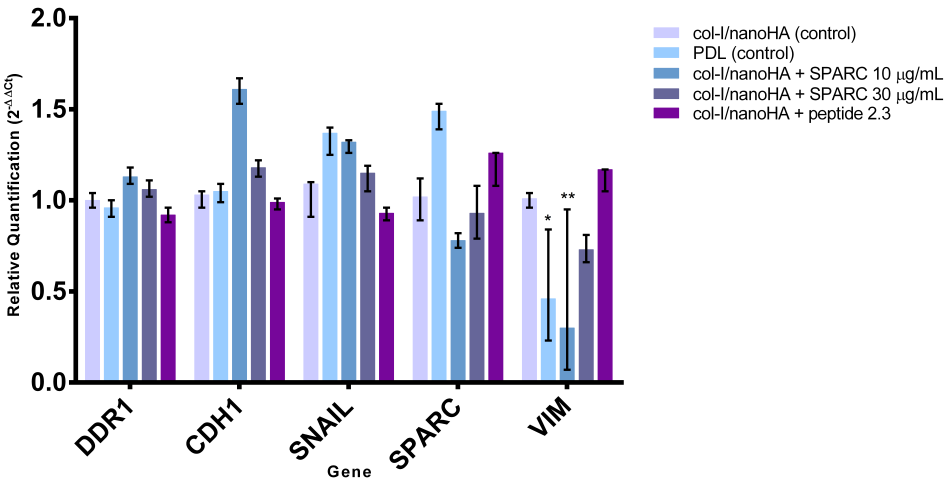

Figure 4.6: Gene expression in relative units for LNCaP monocultures cultured on col-I/nanoHA biocomposite, functionalized with SPARC and SPARC 2.3 peptide, for 5 days: col-I/nanoHA, col-I/nanoHA with SPARC 10 μg/mL, col-I/nanoHA with SPARC 30 μg/mL and col-I/nanoHA with 2.3 peptide 46.2 μg/mL. Monocultures on PDL coated coverglasses were used as positive controls. Monocultures on biocomposite without peptide used as statistical standard. * and ** indicate crescent levels of statistical significance, respectively, $p \leq 0.05$ and $p \leq 0.01$. Graphs and statistical analysis obtained with GraphPad Prism 6 software. *DDR1*, *CDH2* and *SNAIL* expression, *SPARC* and *VIM* expression.

4.5 Endothelial/PCa cells co-cultures

Figure 4.9 shows the gene expression in the endothelial and PCa cells co-cultures, comparing culture in col-I/nanoHA biomaterial with col-I/nanoHA with SPARC 10 μg/mL addition.

Similar to HPMEC-ST1.6R monocultures, both co-cultures did not express *CDH1* and expressed all the other genes.

In Table 4.1 it is summarized the tested genes expression for the HPMEC-ST1.6R and LNCaP monocultures comparing with HPMEC-ST1.6R/LNCaP co-cultures. Although both HPMEC-ST1.6R and LNCaP monocultures did not express *TWIST*, its expression is present in the co-culture. No statistical analysis could be done with these results, due to the lack of data, however, it is possible to observe that the results present a wide variation in value with elevated deviation.

In Table 4.2 it is summarized the tested genes expression for the HPMEC-ST1.6R and PC-3 monocultures comparing with HPMEC-ST1.6R/PC-3 co-cultures. Again, no statistical analysis could be done with these results, however, it is possible to observe that the results present a smaller variation in value with smaller deviation.

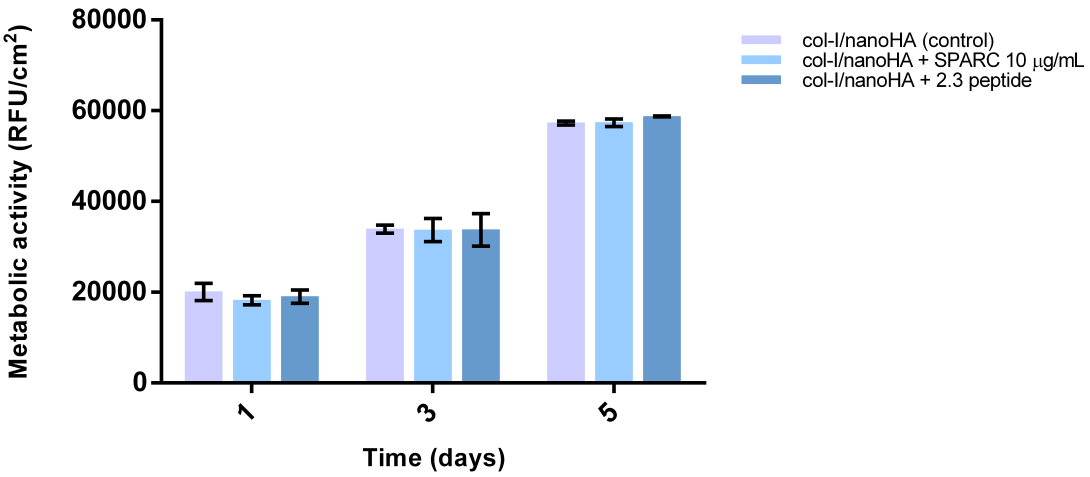

Figure 4.7: Metabolic activity in RFU per cm^2 for PC-3 monocultures cultured on col-I/nanoHA biocomposite, functionalized with SPARC and SPARC peptides, at the end of 1, 3 and 5 days of culture: col-I/nanoHA, col-I/nanoHA with SPARC 10 μg/mL and col-I/nanoHA with peptide 2.3 46.2 μg/mL. Monocultures on biocomposite without peptide used as statistical standard. Results obtained with a Synergy Mx microplate reader. Graphs and statistical analysis obtain with GraphPad Prism 6 software.

4.6 Cell proliferation and morphology

First, the implemented protocol was tested for concentration, namely, of the antibody and the reagent of permeabilization, allowing to decide on the protocol that allowed better visualisation (results not shown).

A 3 days culture of the 3 cell lines in col-I/nanoHA biomaterial was developed and incubated with monoclonal CD31 and DAPI to test the specificity of the monoclonal CD31 antibody. The results of the immunostaining are in Figure 4.10.

As expected, DAPI colouration stained the nucleus in all cell lines but monoclonal CD31 colouration only stained the cytoskeletal of HPMEC-ST1.6R cells. This proves the specificity of monoclonal CD31 for endothelial cells, being adequate for future developments of the work. However, there was possible to observe a high background signal in the unprocessed image revealing that the biomaterial itself has some fluorescence.

A second 3 days culture was conducted for the 3 cell lines with monoclonal CD31 and DAPI for the endothelial cells and AMACR and DAPI for the PCa cells. The results for HPMEC-ST1.6R and LNCaP can be seen in Figure 4.11. For the PC-3 cell line, however, the immunostaining was negative (results not shown).

In this case, it is possible to observe that both antibodies help to locate and limit the morphology of the two different types of cells. Regarding the PC-3 negative result, it reveals that a new protocol optimization is needed for this stage.

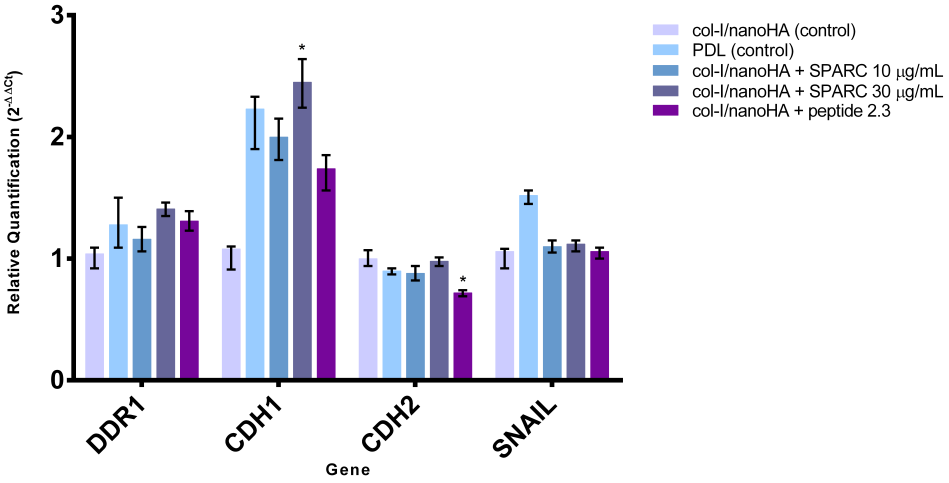

(a)

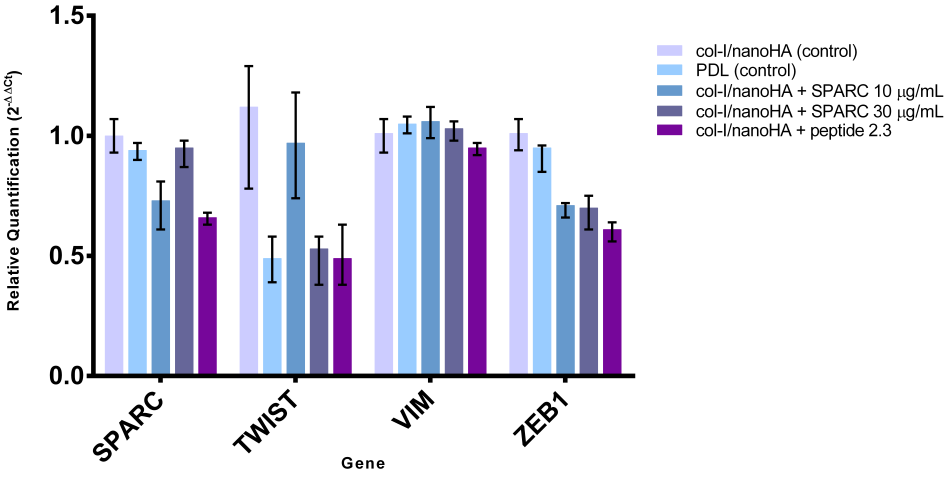

(b)

Figure 4.8: Gene expression in relative units for PC-3 monocultures cultured on col-I/nanoHA biocomposite, functionalized with SPARC and SPARC 2.3 peptide, for 5 days: col-I/nanoHA, col-I/nanoHA with SPARC 10 μg/mL, col-I/nanoHA with SPARC 30 μg/mL and col-I/nanoHA with 2.3 peptide 46.2 μg/mL. Monocultures on PDL coated coverglasses were used as positive controls. Monocultures on biocomposite without peptide used as statistical standard. *, **, ***, **** indicate crescent levels of statistical significance, respectively, $p \leq 0.05$, $p \leq 0.01$, $p \leq 0.001$ and $p \leq 0.0001$. Graphs and statistical analysis obtained with GraphPad Prism 6 software. (a) *DDR1*, *CDH2*, *CDH1* and *SNAIL* expression. (b) *SPARC*, *TWIST*, *VIM* and *ZEB1* expression.

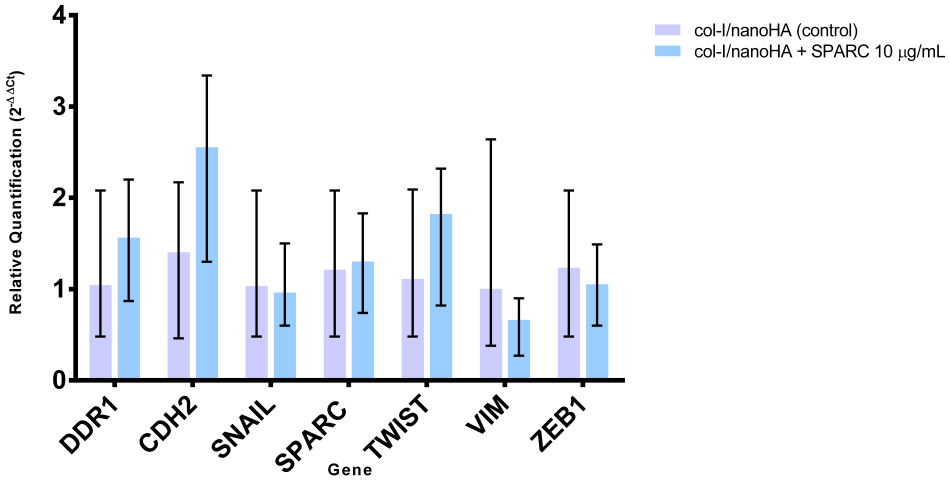

(a)

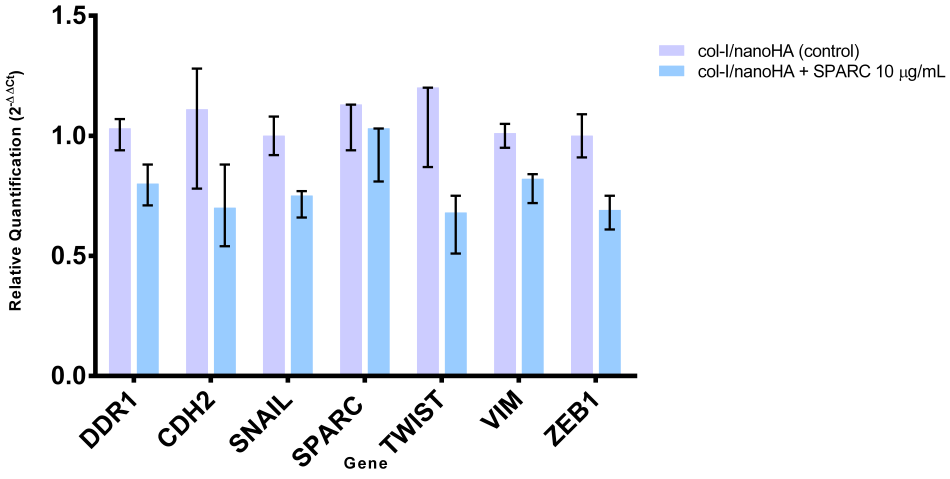

(b)

Figure 4.9: Gene expression in relative units for HPMEC-ST1.6R/PCa cells co-cultures cultured on col-I/nanoHA biocomposite, functionalized with SPARC, for 5 days: col-I/nanoHA and col-I/nanoHA with SPARC 10 μg/mL. Graphs obtained with GraphPad Prism 6 software. *DDR1*, *CDH2*, *SNAIL*, *SPARC*,*TWIST*, *VIM* and *ZEB1* expression. (a) HPMEC-ST1.6R/LNCaP cells co-cultures. (b) HPMEC-ST1.6R/PC-3 cells co-cultures.

Table 4.1: Comparison between gene expression in the HPMEC-ST1.6R and LNCaP monocultures and HPMEC-ST1.6R/LNCaP co-cultures.

	HPMEC-ST1.6R	**LNCaP**	**HPMEC-ST1.6R/LNCaP**
CDH2	Expressed.	Not expressed.	Expressed.
CDH1	Not expressed.	Expressed.	Not expressed.
DDR1	Expressed.	Expressed.	Expressed.
SNAIL	Expressed.	Expressed.	Expressed.
SPARC	Expressed.	Expressed.	Expressed.
TWIST	Not expressed.	Not expressed.	Expressed.
VIM	Expressed.	Expressed.	Expressed.
ZEB1	Expressed.	Not expressed.	Expressed.

Lastly, the experiment was repeated and observed in the LCSM. The results for HPMEC-ST1.6R and LNCaP can be seen in Figure 4.12. Although these results are still preliminary, it is possible to observe the immunostaining with a higher resolution.

Table 4.2: Comparison between gene expression in the HPMEC-ST1.6R and PC-3 monocultures and HPMEC-ST1.6R/PC-3 co-cultures.

	HPMEC-ST1.6R	**PC-3**	**HPMEC-ST1.6R/PC-3**
CDH2	Expressed.	Expressed.	Expressed.
CDH1	Not expressed.	Expressed.	Not expressed.
DDR1	Expressed.	Expressed.	Expressed.
SNAIL	Expressed.	Expressed.	Expressed.
SPARC	Expressed.	Expressed.	Expressed.
TWIST	Not expressed.	Expressed.	Expressed.
VIM	Expressed.	Expressed.	Expressed.
ZEB1	Expressed.	Expressed.	Expressed.

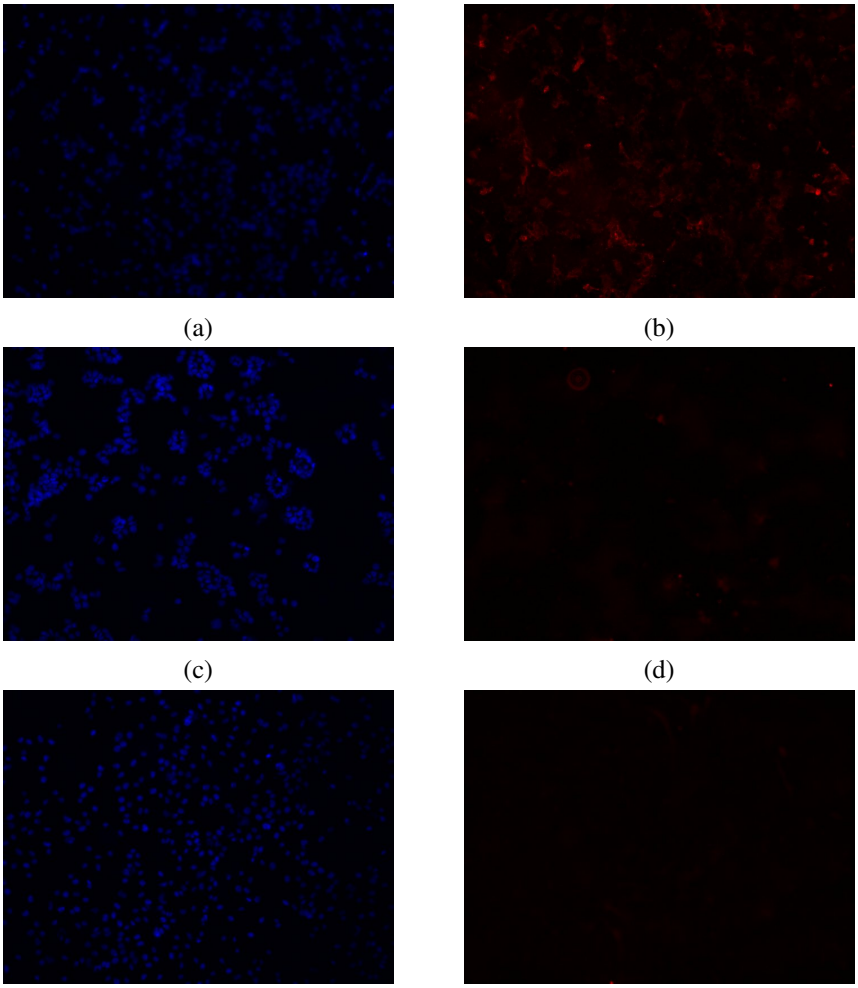

Figure 4.10: IFM images of a 3 days culture of the HPMEC-ST1.6R, LNCaP and PC-3 cell lines on col-I/nanoHA biomaterial. DAPI colouration of the cell nucleus in blue and monoclonal CD31 for endothelial cell cytoskeletal in red. Images obtained in an AxioVert 200 M (Carl Zeiss Microscopy, LLC) and processed with Fiji (ImageJ) software. (a) HPMEC-ST1.6R with DAPI. (b) HPMEC-ST1.6R with monoclonal CD31. (c) LNCaP with DAPI. (d) LNCaP with monoclonal CD31. (e) PC-3 with DAPI. (f) PC-3 with monoclonal CD31.

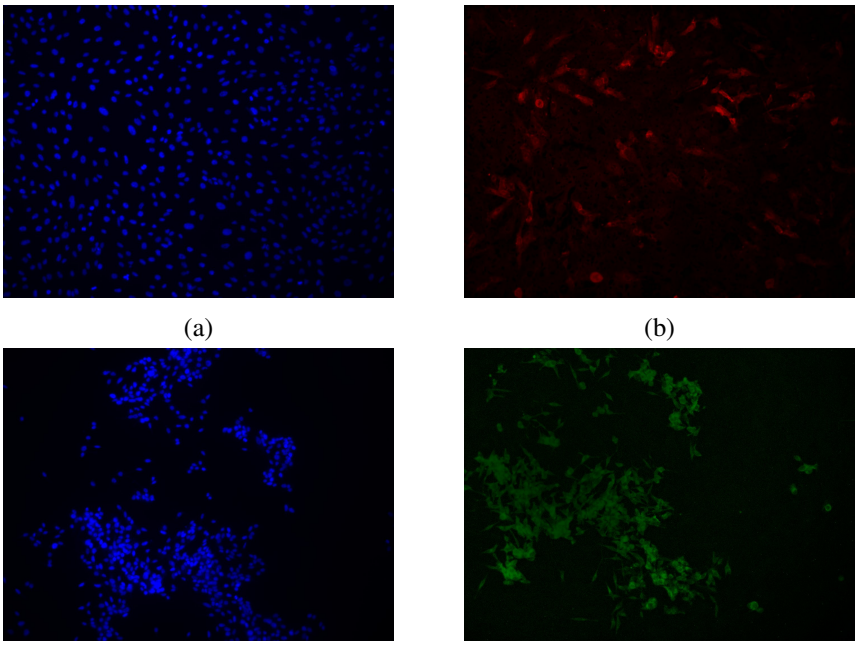

(a) (b)

(c) (d)

Figure 4.11: IFM images of a 3 days culture of the HPMEC-ST1.6R and LNCaP cell lines on col-I/nanoHA biomaterial. DAPI colouration of the cell nucleus in blue, monoclonal CD31 for endothelial cell cytoskeletal in red and AMACR for PCa mitochondria and peroxidases in green. Images obtained in an AxioVert 200 M (Carl Zeiss Microscopy, LLC) and processed with Fiji (ImageJ) software. (a) HPMEC-ST1.6R with DAPI. (b) HPMEC-ST1.6R with monoclonal CD31. (c) LNCaP with DAPI. (d) LNCaP with AMACR.

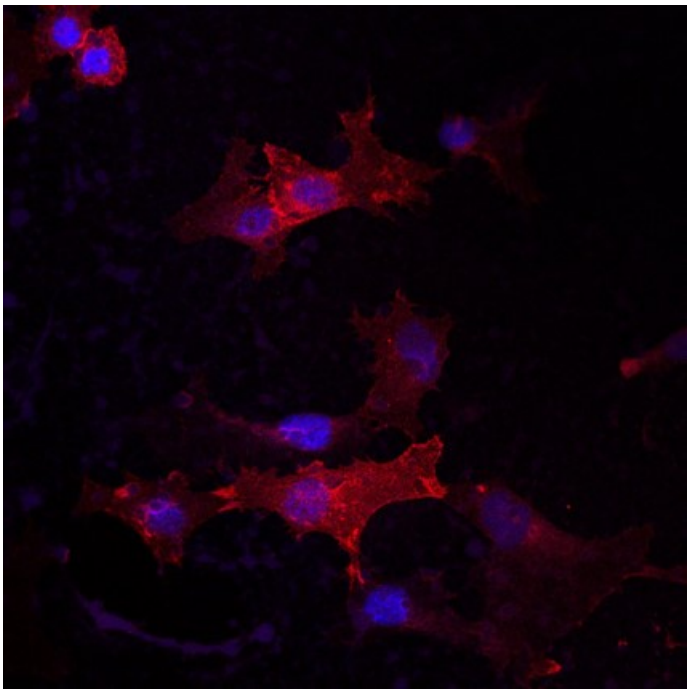

(a)

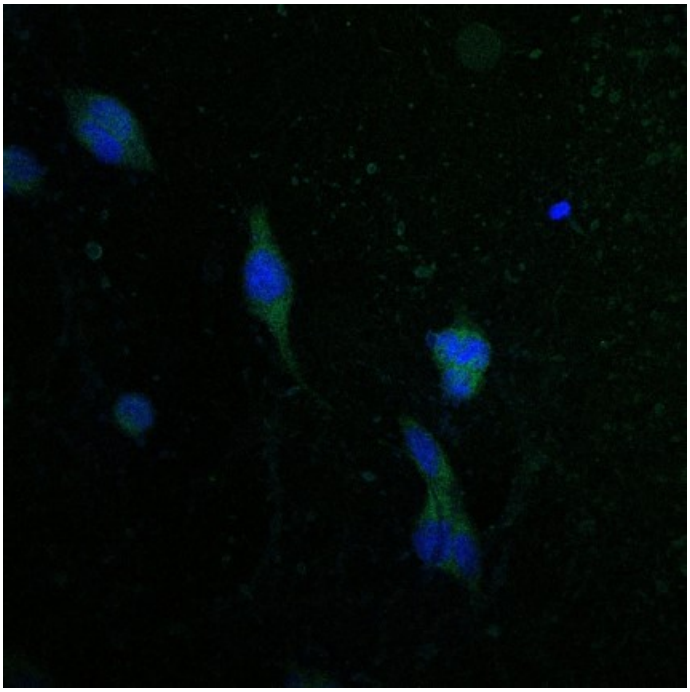

(b)

Figure 4.12: LCSM images of a 3 days culture of the HPMEC-ST1.6R and LNCaP cell lines on col-I/nanoHA biomaterial. DAPI colouration of the cell nucleus in blue, monoclonal CD31 for endothelial cell cytoskeletal in red and AMACR for PCa mitochondria and peroxidases in green. Images obtained in an LCS SP2 AOBS (Leica Microsystems Heidelberg GmbH) and processed with Fiji (ImageJ) software. (a) HPMEC-ST1.6R monoculture. (b) LNCaP monoculture.

Chapter 5

Discussion

The aim of this work was to better understand how SPARC and SPARC derived peptides influence tumorigenesis and PCa osseous metastization by developing *in vitro* endothelial and PCa cells monocultures and co-cultures, in a bone biomimetic biomaterial. For that reason, one endothelial (HPMEC-ST1.6R) and two PCa (LNCaP and PC-3) cell lines were elected and metabolic activity was assessed with a resazurin assay, EMT related gene expression was assessed with real time RT-PCR and an immunostaining protocol was implemented for accessing morphology.

Regarding metabolic activity, the exogenous SPARC and SPARC 2.3 peptide addition seem to induce HPMEC-ST1.6R proliferation at the end of 5 days. This is consistent with the literature that indicates that SPARC can regulate endothelial proliferation and promote angiogenesis and also that 2.3 peptide has a positive effect on endothelial cell proliferation [11, 44–46].

For the LNCaP cell line, SPARC seems to have an inhibitory effect in metabolic activity while the 2.3 peptide seems to behave in the opposite way. It is interesting to note that regarding this last case, the augment in proliferation is only possible to observe at the end of 3 culture days. Since LNCaP is a cell line that grows in clusters, confluency and a plateau phase in proliferation are achieved quickly. This way, it might be an interesting approach to reduce the time points, to achieve a more statistically significant results variation.

For the PC-3 cell line, no influence can be detected in the metabolic activity after the exogenous SPARC addition, being this result consistent with the fact that this cell line has a natural high SPARC expression and production [50].

Regarding the gene expression on the col-I/nanoHA biomaterial comparing with the positive control (Table B.1), some general analysis can be made. For instance, the expression of *VIM* in the biomaterial was higher than in the control, both for LNCaP and HPMEC-ST1.6R. Challa and Stefanovic [63] may explain it: VIM seems to play a role in binding and stabilisation of mRNAs of col-I. Thus, it seems logical that these cells have increased production, in a col-I rich environment. PC-3 already has a natural high col-I affinity, which may explain why the expression is constant.

DDR1 and *SPARC* also showed higher expression levels in the biomaterial, for HPMEC-ST1.6R, which is consistent with the literature, since both have col-I affinity. The biomaterial seemed to induce in HPMEC-ST1.6R expression of genes that induce a mesenchymal phenotype:

CDH2, *ZEB1* and *VIM*. This might imply that EMT is naturally promoted in endothelial cells when introduced to a bone mimetic microenvironment.

Regarding the gene expression for the other conditions (Table B.2), in general, the addition of SPARC and 2.3 peptide, with the chosen concentrations, lead to a general decrease of genes that induce EMT and an increase of the one that is negative related with the transition; in other words, it seems to have induced an epithelial phenotype. This was particularly significant for the HPMEC-ST1.6R cell line. Thus, the results point towards an inhibitory effect of the EMT process caused by the addition of exogenous SPARC and 2.3 peptide, which can be related to an inhibition of the potential for angiogenesis and tumour migration.

Approaching now the gene expression results for the co-cultures, it is interesting to notice that HPMEC-ST1.6R seems to dictate the lack of the epithelial cadherin expression in the co-cultures, although this was not true for the *TWIST* gene. As seemed before, Twist is expressed as a result of hypoxia and upregulates *CDH2*, activates *SPARC* and is related to several types of cancer [17,21]. This way, it is possible to formulate that perhaps the cellular overgrowth of the co-culture leads to hypoxia and activates *TWIST* expression, even if it was not present in the monocultures. This formulation is also consistent with the fact that, on the monocultures, *TWIST* is only expressed in PC-3, a cell line with high proliferation on a bone mimetic environment.

Regarding the above results, although no statistical analysis can be made at this point, in the HPMEC-ST1.6R/PC-3 co-cultures it is possible to observe an inhibition of the pro-EMT genes with the addition of SPARC, in the same way as the monocultures. For the HPMEC-ST1.6R/LNCaP co-cultures, as said before, the results seem very inconsistent, with no specific tendency and an elevated standard deviation, been necessary further developments in order to make any conclusions.

Lastly, the conducted immunostaining experiences had as propose to understand if this approach can be applied to observe cell proliferation and morphology in co-cultures, with different culture conditions. Monoclonal CD31 was proved to be a good choice to mark endothelial cells, showing no false positives and delimiting unambiguously the cellular structure.

AMACR, although it is a very well know PCa antibody and used in the daily practice, failed to do so for the PC-3 cell line. This could be explained by the fact that PC-3 has natural lower expression of the marker [40] and that a new protocol optimization is needed. However, an alternative may be used, for instance, a CellTracker^{TM} fluorescent probe: these probes allow to control cellular proliferation of a specific cell line since, once living cells are stained, the fluorescence is retained for several generations, being transferred to daughter cells but not adjacent cells in a population. As an advantage, they can be used to co-staining with antibodies or another type of probes, so it would be appropriate for co-cultures [64].

Chapter 6

Conclusions

Although PCa mortality rates have been steady, mainly in the developed world, due to early diagnosis [6], bone metastatic PCa is still a disease without a cure. Hence, it is imperative to build adequate models and study hypothesis that help to unravel the mechanisms beyond bone metastization.

Angiogenesis is a hallmark of cancer and EMT is an angiogenesis-related process that is thought to play an important part in metastization. The occurrence of EMT is in an intimate relationship with the microenvironment, namely, the presence of certain transcription factors. This way, these transcription factors and other proteins associated with EMT can be used as biomarkers of the metastization potential.

SPARC seems to play crucial, yet not totally understood, role in several processes including bone remodelling, angiogenesis and tumour progression. In its structure, it contains several bioactive peptides, like 2.3 peptide, that is pro-angiogenic, promoting endothelial cell proliferation, and 4.2 peptide, which stimulates endothelial cells migration without stimulating its proliferation.

Regarding PCa, SPARC may function as a tumour biomarker and a tumour suppressor. SPARC is overexpressed in metastatic PCa cells and in bone metastases, hence, the potential for becoming a biomarker. However, the most aggressive PCa tumours seem to be the ones that have the lowest levels of SPARC, indicating that SPARC may have a certain inhibitory effect. Also, being bone metastization associated with irregular bone remodelling, it is easy to understand that SPARC may help to prevent PCa expansion in the bone.

An endothelial cell line, HPMEC-ST1.6R, and two PCa cell lines, a bone metastatic and a non-bone metastatic line, PC-3 and LNCaP, were cultured in a bone biomimetic biocomposite. Metabolic activity was accessed at the end of 1, 3 and 5 days, in the presence and absence of SPARC 10 μg/mL and SPARC 2.3 peptide. In endothelial cells, SPARC and its peptide both induced cell proliferation. In LNCaP, SPARC acted as a suppressor however the 2.3 peptide leads to increased proliferation. In PC-3, no changes could be detected, since this cell line already has a very high proliferation in a bone biomimetic environment.

SPARC 4.2 peptide was optimized for concentration: several concentrations were added to the biocomposite of an endothelial monoculture and it was revealed that 230 μM was the ideal

condition to develop future and similar studies regarding this peptide.

Gene expression of genes related with EMT, namely *DDR1*, *CDH1*, *CDH2*, *SNAIL*, *SPARC*, *TWIST*, *VIM* and *ZEB1*, was also access at the end of 5 culture days, in the same monoculture conditions but also for endothelial/PCa cells co-cultures. Regarding the monocultures, the endothelial cells revealed higher expression of EMT related genes in the biocomposite when compared with a positive control. This seems to be related to the col-I affinity these factors have, helping the endothelial cells to proliferate in the new environment. This phenomenon could also be seen in LNCaP monocultures but was not relevant for PC-3 since this cell line has a naturally high affinity to col-I.

The addition of exogenous SPARC 10 μg/mL, SPARC 30 μg/mL and 2.3 peptide to the biocomposite lead to a decreased in the expression of EMT related genes, by all the monocultures cells lines. This is congruent with the idea of SPARC working as a tumour suppressor in PCa. Regarding the co-cultures, the results seemed to follow the same tendency in HPMEC-ST1.6R/PC-3 co-cultures, however, more studies will be necessary to present more solid conclusions.

Lastly, monoclonal CD31 and AMACR were tested as biomarkers to access co-culture cell morphology and proliferation, using IFM and LCSM. CD31 revealed to be an appropriated and specific endothelial marker, however, AMACR failed to mark PC-3 cells. Further protocol optimization may be needed since it is well known that PC-3 has a lower AMACR expression than LNCaP, where the immunostaining seemed to have worked. Adding to this, the biocomposite revealed to have some fluorescence, producing a background signal that needs to be taken into consideration.

Chapter 7

Future Work

In this dissertation, endothelial and PCa cells monocultures and co-cultures were conducted in a bone biomimetic material, in the presence or absence of SPARC and SPARC peptides, in order to better understand SPARC influence in PCa bone metastization. Therefore, to continue throughways the same aim of work, future work will have to include further essays regarding metabolic activity, gene expression and morphology assessment.

The endothelial/PCa co-culture model is very important to understand the SPARC influence in PCa angiogenesis in a bone microenvironment. Further essays regarding metabolic activity and gene expression are needed, in order to be compared with the already obtained results for the monocultures, presenting solid conclusions. Also, since the 4.2 peptide was optimized for concentration, it is now possible to introduce a new culture condition for all the essays presented before.

A new cell line can be introduced to the experiment, namely, an osteoblastic cell line. MC3T3-E1 is a clonal osteogenic cell line derived from newborn mouse calvaria that has high alkaline phosphatase activity after reaching a confluent state. These cells have the ability to present *in vitro* differentiation into osteoblasts, which make them a useful model [65]. Monocultures similar to the ones presented before can be conducted. A co-culture model of osteoblasts and PCa cells can also be developed by seeding osteoblasts in the biocomposite and, subsequently, PCa cells, creating a simulation of metastatic tissue.

Regarding morphology assessment, after the already mentioned immunostaining protocol optimisation, monocultures of endothelial and PCa cells lines can be observed and compared at the end of different time points, with different culture conditions. The same can be applied to the co-cultures, using a combined immunostaining protocol, with monoclonal CD31 and AMACR. For the osteoblasts/PCa co-cultures, an approach like the CellTracker^{TM} fluorescent probes could be an easy way to obtain good results.

Lastly, in a more distant future, instead of studying the influence of exogenous peptides, it would be a different and interesting approach to study the manipulation of the peptides endogenous expression and production. All these hypotheses combined would provide further information regarding the search for a new and effective way to battle bone metastatic prostate cancer.

Appendix A

Recent studies regarding PCa and SPARC

Table A.1: Most revelant studies regarding PCa and SPARC from 2016 to 2018, the models used and its main conclusions.

Study	Models	Main conclusions
Ribeiro *et al.* [50]	*In vitro* 3D bone biomimetic model and *ex vivo* samples: primary tumours from 194 patients, 27 prostatic intraepithelial neoplasia's and 15 morphologically normal prostate tissues.	*In vitro* model: SPARC addition contributed to the survival and significant growth of a non-bone metastatic PCa cell line (LNCaP). *Ex vivo*: there were higher SPARC levels in cells from patients with higher Gleason Score, which indicates tumours with a poorer prognosis, as well as cells from metastasis, particularly from bone sites, compared with regular PCa cells.
Sharma *et al.* [66]	*In vivo* selection by implanting PC3mm stem-like cells into tibial bones of nude mice.	Indolent PCa cells have a high expression of SPARC that leads to the secretion of BMP7, that keeps the cells in a dormant-like stage, in the bone microenvironment. Aggressive PCa cells have SPARC epigenetically silenced by promoter methylation.

Windrichova *et al.* [67] and Windrichova *et al.* [68]	*Ex vivo* samples: 62 oncological patients, including patients with the following diagnosis: prostate cancer, breast cancer, lung cancer and colorectal cancer.	SPARC is tested as a bone-metastatic biomarker, for several types of cancer, and it is concluded that it has potential, since higher levels of SPARC were found in patients with metastases. This leads that SPARC, joining with other biomarkers, is integrated into a formula to calculate the potential of metastization, using a multivariate logistic regression model, in order to improve early diagnosis.
Chen *et al.* [69]	*In vivo* testing with mice and *ex vivo* samples: 50 oncological patients.	SPOCK1, a proteoglycan of the family of SPARC, is proven to have an active part in PCa proliferation. The introduction of SPOCK1 free PCa cells leads to low metastization, cell cycle arrest in G0/G1 phase and even apoptotic processes (death of the PCa cells).
Katafigioti *et al.* [70]	Urine samples of 127 patients	SPARC as a PCa biomarker is included in a urine test, however, it does not reveal to be an efficient indicator.
Georgescu *et al.* [71]	*Ex vivo* samples: 41 oncological patients with higher classification in the Gleason scale.	SPARC as other biomarkers may be used to improve the Gleason scale in the distinction of the most aggressive types of PCa cancer. SPARC revealed to be upregulated in the most aggressive types.
Sung *et al.* [72]	*In vitro* with no biomaterial support, *in vivo* with nude mice and also *ex vivo* samples.	SPARC is chosen as a target for gene therapy since is present both in tumour epithelial cells and bone cells: a SPARC promoter could be used to target both bone metastatic PCa and its supporting microenvironment, that the cancer cells need to survive.
Cruz-Neves *et al.* [51]	3D bone-like *in vitro* model.	The external adding of SPARC to non-bone metastatic PCa cells leads to the proliferation of the cells in bone microenvironment; however, when the same is done to bone metastatic cells, there is no significant difference.
Gagliardi *et al.* [73]	(review article)	SPARCL1, a protein of the SPARC family is proven to be sub-expressed in PCa cells: its presence revealed to suppress PCa metastization and migration.

Okato *et al.* [74] and Yamada *et al.* [75]	*Ex vivo* samples and *in vitro* with no biomaterial support.	The inhibitory potential of SPARC by microRNAs is studied. MicroRNAs are proved to be crucial in the proliferation of PCa: high levels of SPARC results in low levels of microRNAs and this conducts to cancer proliferation. Since the way around is also true, high levels of microRNAs result in SPARC levels reduction: inducing proliferation of microRNAs leads to low levels of SPARC and PCa metastization.
Liu *et al.* [76]	*Ex vivo* samples: 207 prostate samples; and *in vitro* with no biomaterial support.	It was concluded that the expression of the gene that leads to the production of SPARC is decreased in PCa cells and that this is related to the hypermethylation of this gene. Thus, the access of this hypermethylation can be a potential biomarker for poor prognosis in PCa patients.
Shkurnikov *et al.* [77]	*Ex vivo* samples.	It was suggested that the extracellular matrix components surrounding lymph nodes affected by PCa metastases, such as SPARC, were affected, having a decreased of its levels.
Hao *et al.* [78]	*Ex vivo* samples: 72 prostate samples; and *in vitro* with no biomaterial support.	MicroRNA miR-211 is downregulated in PCa cells and target SPARC, which is upregulated in PCa cells.

Appendix B

Gene expression on monocultures

Table B.1: Comparison between gene expression in relative units for the 3 cell lines in the col-I/nanoHA biocomposite and PDL control. *, **, *** and **** indicates crescent levels of statistical significance, respectively, $p \leq 0.05$, $p \leq 0.01$, $p \leq 0.001$ and $p \leq 0.0001$.

	PC-3	**LNCaP**	**HPMEC-ST1.6R**
CDH2	No difference.	Null expression.	Higher expression on biomaterial (**).
CDH1	No difference.	No difference.	Null expression.
TWIST	No difference.	Null expression.	Null expression.
ZEB1	No difference.	Null expression.	Higher expression on biomaterial (**).
VIM	No difference.	Higher expression on biomaterial (*).	Higher expression on biomaterial (****).
SNAIL	No difference.	No difference.	No difference.
DDR1	No difference.	No difference.	Higher expression on biomaterial (**).
SPARC	No difference.	No difference.	Higher expression on biomaterial (**).

Table B.2: Comparison between gene expression for the 3 cell lines in biomaterial with col-1/nanoHA biomaterial with SPARC 10 μL/mL, with SPARC 30 μL/mL and with 2.3 peptide. *, **, *** and **** indicates crescent levels of statistical significance, respectively, $p \leq 0.05$, $p \leq 0.01$, $p \leq 0.001$ and $p \leq 0.0001$.

	PC-3			LNCaP			HPMEC-ST1.6R		
	SPARC 10 μL/mL	**SPARC 30 μL/mL**	**2.3 peptide**	**SPARC 10 μL/mL**	**SPARC 30 μL/mL**	**2.3 peptide**	**SPARC 10 μL/mL**	**SPARC 30 μL/mL**	**2.3 peptide**
CDH2	No difference.	No difference.	Decreased expression (*).	Null expression.	Null expression.	Null expression.	Decreased expression (**).	Decreased expression (*).	Decreased expression (**).
CDH1	No difference.	Increased expression (*).	No difference.	No difference.	No difference.	No difference.	Null expression.	Null expression.	Null expression.
TWIST	No difference.	No difference.	No difference.	Null expression.	Null expression.	Null expression.	Null expression.	Null expression.	Null expression.
ZEB1	No difference.	No difference.	No difference.	Null expression.	Null expression.	Null expression.	Decreased expression (**).	Decreased expression (*).	Decreased expression (***).
VIM	No difference.	No difference.	No difference.	Decreased expression (**).	No difference.	No difference.	Decreased expression (****).	Decreased expression (**).	Decreased expression (****).
SNAIL	No difference.	No difference.	No difference.	No difference.	No difference.	No difference.	No difference.	No difference.	No difference.
DDR1	No difference.	No difference.	No difference.	No difference.	No difference.	No difference.	Decreased expression (*).	No difference.	No difference.
SPARC	No difference.	No difference.	No difference.	No difference.	No difference.	No difference.	Decreased expression (*).	Decreased expression (**).	Decreased expression (*).

References

[1] Cancer Research UK. What is cancer? [Online]. URL: https://www.cancerresearchuk.org/about-cancer/what-is-cancer [last accessed 2020-01-16].

[2] Rod R. Seeley. *Anatomia & Fisiologia*. Lusociência - Edições Técnicas e Científicas, 6th edition, 2003.

[3] American Cancer Society. Prostate Cancer [Online]. URL: https://www.cancer.org/cancer/prostate-cancer/ [last accessed 2020-01-16].

[4] Eugene Pietzak and Phillip Mucksavage. Chapter 53 - Bone Health in Prostate Cancer. In *Prostate Cancer: Science and Clinical Practice*, pages 491–507. Academic Press, 2th edition, 2016. doi:10.1016/B978-0-12-800077-9.00053-0.

[5] Sok Kuan Wong, Nur-Vaizura Mohamad, Tijjani Rabiu Giaze, Kok-Yong Chin, Norazlina Mohamed, and Soelaiman Ima-Nirwana. Prostate Cancer and Bone Metastases: The Underlying Mechanisms. *International Journal of Molecular Sciences*, 20(10):2587, 2019. doi:10.3390/ijms20102587.

[6] Freddie Bray, Jacques Ferlay, Isabelle Soerjomataram, Rebecca L. Siegel, Lindsey A. Torre, and Ahmedin Jemal. Global cancer statistics 2018: GLOBOCAN estimates of incidence and mortality worldwide for 36 cancers in 185 countries. *CA: A Cancer Journal for Clinicians*, 68(6):394–424, 2018. doi:10.3322/caac.21492.

[7] The Global Cancer Observatory. Portugal - Global Cancer Observatory, 2019. URL: http://gco.iarc.fr/today/data/factsheets/populations/620-portugal-fact-sheets.pdf.

[8] American Cancer Society. Cancer Facts & Figures 2017, 2017. URL: https://www.cancer.org/content/dam/cancer-org/research/cancer-facts-and-statistics/annual-cancer-facts-and-figures/2017/cancer-facts-and-figures-2017.pdf.

[9] Lukas Bubendorf, Alain Schöpfer, Urs Wagner, Guido Sauter, Holger Moch, Niels Willi, Thomas C. Gasser, and Michael J. Mihatsch. Metastatic patterns of prostate cancer: An autopsy study of 1,589 patients. *Human Pathology*, 31(5):578–583, 2000. doi:10.1053/hp.2000.6698.

[10] E. David Crawford, Karen H. Ventii, and Neal D. Shore. Chapter 66 - New Markers for Prostate Cancer Detection and Prognosis. In *Prostate Cancer: Science and Clinical Practice*, pages 623–632. Academic Press, 2th edition, 2016. doi:10.1016/B978-0-12-800077-9.00066-9.

[11] Nilza Ribeiro, Susana R. Sousa, Rolf A. Brekken, and Fernando J. Monteiro. Role of SPARC in Bone Remodeling and Cancer-Related Bone Metastasis. *Journal of Cellular Biochemistry*, 115(1):17–26, 2014. doi:10.1002/jcb.24649.

[12] Nilza Ribeiro, Susana R. Sousa, Clemens A. van Blitterswijk, Lorenzo Moroni, and Fernando J. Monteiro. A biocomposite of collagen nanofibers and nanohydroxyapatite for bone regeneration. *Biofabrication*, 6(3), 2014. doi:10.1088/1758-5082/6/3/035015.

[13] Anna Dimberg and Malin Sund. Cancer Angiogenesis and Vasculogenesis. In *Pathobiology of Human Disease: A Dynamic Encyclopedia of Disease Mechanisms*, pages 403–411. Academic Press, 2014. doi:10.1016/B978-0-12-386456-7.01908-0.

[14] Naoyo Nishida, Hirohisa Yano, Takashi Nishida, Toshiharu Kamura, and Masamichi Kojiro. Angiogenesis in Cancer. *Vascular Health and Risk Management*, 2(3):213–9, 2006. URL: http://www.pubmedcentral.nih.gov/articlerender.fcgi?artid=PMC1993983, doi:10.2147/vhrm.2006.2.3.213.

[15] Shaker A. Mousa and Paul J. Davis. Chapter 1 - Angiogenesis and Anti-Angiogenesis Strategies in Cancer. In *Anti-Angiogenesis Strategies in Cancer Therapeutics*, pages 1–19. Academic Press, 2017. doi:10.1016/B978-0-12-802576-5.00001-2.

[16] Raghu Kalluri and Robert A. Weinberg. The basics of epithelial-mesenchymal transition. *Journal of Clinical Investigation*, 119(6):1420–1428, 2009. doi:10.1172/JCI39104.

[17] Samy Lamouille, Jian Xu, and Rik Derynck. Molecular mechanisms of epithelial-mesenchymal transition. *Nature Reviews Molecular Cell Biology*, 15(3):178–196, 2014. doi:10.1038/nrm3758.

[18] Krzysztof Marek Mrozik, Orest William Blaschuk, Chee Man Cheong, Andrew Christopher William Zannettino, and Kate Vandyke. N-cadherin in cancer metastasis, its emerging role in haematological malignancies and potential as a therapeutic target in cancer. *BMC Cancer*, 18:939, 2018. doi:10.1186/s12885-018-4845-0.

[19] Arun Satelli and Shulin Li. Vimentin in cancer and its potential as a molecular target for cancer therapy. *Cellular and Molecular Life Sciences*, 68(18):3033–3046, 2011. doi:10.1007/s00018-011-0735-1.

[20] E. Sánchez-Tilló, A. Lázaro, R. Torrent, M. Cuatrecasas, E. C. Vaquero, A. Castells, P. Engel, and A. Postigo. ZEB1 represses E-cadherin and induces an EMT by recruiting the SWI/SNF chromatin-remodeling protein BRG1. *Oncogene*, 29:3490–2500, 2010. doi:10.1038/onc.2010.102.

[21] Md. Asaduzzaman Khan, Han-chun Chen, Dianzheng Zhang, and Junjiang Fu. Twist: a molecular target in cancer therapeutics. *Tumor Biology*, 34(5):2497–2506, 2013. doi:10.1007/s13277-013-1002-x.

[22] Nancy E. Davidson and Saraswati Sukumar. Of Snail, mice, and women. *Cancer Cell*, 8(3):173–174, 2005. doi:10.1016/j.ccr.2005.08.006.

[23] Hong-Ru Chen, Yi-Chun Yeh, Ching-Yi Liu, Yu-Ting Wu, Fang-Yu Lo, Ming-Jer Tang, and Yang-Kao Wang. DDR1 promotes E-cadherin stability via inhibition of integrin-β1-Src activation-mediated E-cadherin endocytosis. *Scientific Reports*, 6:36336, 2016. doi:10.1038/srep36336.

[24] Gunjan Agarwal, Cosmin Mihai, and Daniel F. Iscru. Interaction of Discoidin Domain Receptor 1 with Collagen type 1. *Journal of Molecular Biology*, 367(2):443–455, 2007. doi:10.1016/j.jmb.2006.12.073.

[25] Keiji Shimada, Mitsutoshi Nakamura, Eiwa Ishida, Tomonori Higuchi, Hiroshi Yamamoto, Kazutake Tsujikawa, and Noboru Konishi. Prostate cancer antigen-1 contributes to cell survival and invasion though discoidin receptor 1 in human prostate cancer. *Cancer Science*, 99(1):39–45, 2008. doi:10.1111/j.1349-7006.2007.00655.x.

[26] Yu Zheng, Hong Zhou, Colin R. Dunstan, Robert L. Sutherland, and Markus J. Seibel. The role of the bone microenvironment in skeletal metastasis. *Journal of Bone Oncology*, 2(1):47–57, 2013. doi:10.1016/j.jbo.2012.11.002.

[27] Jia Peng and Yibin Kang. The Bony Side of Endothelial Cells in Prostate Cancer. *Developmental Cell*, 41(5):451–452, 2017. doi:10.1016/j.devcel.2017.05.015.

[28] Andrea I. Alford, Kenneth M. Kozloff, and Kurt D. Hankenson. Extracellular matrix networks in bone remodeling. *The International Journal of Biochemistry & Cell Biology*, 65:20–31, 2015. doi:10.1016/j.biocel.2015.05.008.

[29] Song-Chang Lin, Yu-Chen Lee, Guoyu Yu, Chien-Jui Cheng, Xin Zhou, Khoi Chu, Monzur Murshed, Nhat-Tu Le, Laura Baseler, Jun-ichi Abe, Keigi Fujiwara, Benoit DeCrombrugghe, Christopher J. Logothetis, Gary E. Gallick, Li-Yuan Yu-Lee, Sankar N. Maity, and Sue-Hwa Lin. Endothelial-to-Osteoblast Conversion Generates Osteoblastic Metastasis of Prostate Cancer. *Developmental Cell*, 41(5):467–480, 2017. doi:10.1016/j.devcel.2017.05.005.

[30] Elizabeth A. Zimmermann, Björn Busse, and Robert O. Ritchie. The fracture mechanics of human bone: influence of disease and treatment. *BoneKEy Reports*, 4:743, 2015. doi:10.1038/bonekey.2015.112.

[31] Emilie M. Rosset and Amy D. Bradshaw. SPARC/osteonectin in mineralized tissue. *Matrix Biology*, 52-54:78–87, 2016. doi:10.1016/j.matbio.2016.02.001.

[32] Molly M. Stevens and Julian H. George. Exploring and Engineering the Cell Surface Interface. *Science*, 310(5751):1135–1138, 2005. doi:10.1126/science.1106587.

[33] Anatol Jaworek. Micro- and nanoparticle production by electrospraying. *Powder Technology*, 176(1):18–35, 2007. doi:10.1016/j.powtec.2007.01.035.

[34] Anatol Jaworek and Arkadiusz Tomasz Sobczyk. Electrospraying route to nanotechnology: An overview. *Journal of Electrostatics*, 66(3-4):197–219, 2008. doi:10.1016/j.elstat.2007.10.001.

[35] Dan Li and Younan Xia. Electrospinning of Nanofibers: Reinventing the Wheel? *Advanced Materials*, 16(14):1151–1170, 2004. doi:10.1002/adma.200400719.

[36] Nandana Bhardwaj and Subhas C. Kundu. Electrospinning: A fascinating fiber fabrication technique. *Biotechnology Advances*, 28(3):325–347, 2010. doi:10.1016/j.biotechadv.2010.01.004.

[37] Fernando J. Monteiro, Susana R. Sousa, Nilza Ribeiro, and Lorenzo Moroni. Mesh Composition for Repairing or the Regeneration of Tissues and Methods Thereof, 2015. URL: http://www.sumobrain.com/patents/WO2015162559A1.html.

[38] R. E. Sobel and M. D. Sadar. Cell Lines Used in Prostate Cancer Research: a Compendium of Old and New Lines - Part 1. *The Journal of Urology*, 173(2):342–359, 2005. doi:10.1097/01.ju.0000141580.30910.57.

[39] Ediz Sariisik, Denitsa Docheva, Daniela Padula, Cvetan Popov, Jan Opfer, Matthias Schieker, Hauke Clausen-Schaumann, and Martin Benoit. Probing the Interaction Forces of Prostate Cancer Cells with Collagen I and Bone Marrow Derived Stem Cells on the Single Cell Level. *PLOS ONE*, 8(3):1–11, 2013. doi:10.1371/journal.pone.0057706.

[40] Rainer Kuefer, Sooryanarayana Varambally, Ming Zhou, Peter C. Lucas, Martin Loeffler, Hubertus Wolter, Torsten Mattfeldt, Richard E. Hautmann, Juergen E. Gschwend, Terrence R. Barrette, Rodney L. Dunn, Arul M. Chinnaiyan, and Mark A. Rubin. α-Methylacyl-CoA Racemase: Expression Levels of this Novel Cancer Biomarker Depend on Tumor Differentiation. *American Journal of Pathology*, 161(3):841–848, 2002. doi:10.1016/S0002-9440(10)64244-7.

[41] A. Al-Soudi, M. H. Kaaij, and S. W. Tas. Endothelial cells: From innocent bystanders to active participants in immune responses. *Autoimmunity Reviews*, 16(9):951–962, 2017. doi:10.1016/j.autrev.2017.07.008.

[42] Ronald E. Unger, Vera Krump-Konvalinkova, Kirsten Peters, and C. James Kirkpatrick. *In Vitro* Expression of the Endothelial Phenotype: Comparative Study of Primary Isolated Cells and Cell Lines, Including the Novel Cell Line HPMEC-ST1. 6R. *Microvascular Research*, 64(3):384–397, 2002. doi:10.1006/mvre.2002.2434.

[43] John D. Termine, Hynda K. Kleinman, S. William Whitson, Kathleen M. Conn, Mary L. McGarvey, and George R. Martin. Osteonectin, a bone-specific protein linking mineral to collagen. *Cell*, 26(1):99–105, 1981. doi:10.1016/0092-8674(81)90037-4.

[44] Christine Kupprion, Kouros Motamed, and E. Helene Sage. SPARC (BM-40, Osteonectin) Inhibits the Mitogenic Effect of Vascular Endothelial Growth Factor on Microvascular Endothelial Cells. *Journal of Biological Chemistry*, 273(45):29635–29640, 1998. doi:10.1074/jbc.273.45.29635.

[45] Alexandre Chlenski, Shuqing Liu, Lisa J. Baker, Qiwei Yang, Yufeng Tian, Helen R. Salwen, and Susan L. Cohn. Neuroblastoma Angiogenesis Is Inhibited with a Folded Synthetic Molecule Corresponding to the Epidermal Growth Factor-Like Module of the Follistatin Domain of SPARC. *Cancer Research*, 64(20):7420–7425, 2004. doi:10.1158/0008-5472.CAN-04-2141.

[46] Isabella T. Tai and Michelle J. Tang. SPARC in cancer biology: Its role in cancer progression and potential for therapy. *Drug Resistance Updates*, 11(6):231–246, 2008. doi:10.1016/j.drup.2008.08.005.

[47] A. M. Delany, M. Amling, M. Priemel, C. Howe, R. Baron, and E. Canalis. Osteopenia and decreased bone formation in osteonectin-deficient mice. *The Journal of Clinical Investigation*, 105(7):915–923, 2000. doi:10.1172/JCI7039.

[48] Shuang Zhao, Qianqian Yu, Jiali Pan, Yanhui Zhou, Chengwen Cao, Jian-Ming Ouyang, and Jie Liu. Redox-responsive mesoporous selenium delivery of doxorubicin targets MCF-7 cells and synergistically enhances its anti-tumor activity. *Acta Biomaterialia*, 54:294–306, 2017. doi:10.1016/j.actbio.2017.02.042.

[49] Yu-Jing He, Lei Xing, Peng-Fei Cui, Jia-Liang Zhang, Yong Zhu, Jian-Bin Qiao, Jin-Yuan Lyu, Mei Zhang, Cheng-Qiong Luo, Yu-Xin Zhou, Na Lu, and Hu-Lin Jiang. Transferrin-inspired vehicles based on pH-responsive coordination bond to combat multidrug-resistant breast cancer. *Biomaterials*, 113:266–78, 2017. doi:10.1016/j.biomaterials.2016.11.001.

[50] Nilza Ribeiro, Pedro Costa-Pinheiro, Rui Henrique, Maria Gomez-Lazaro, Marisa P. Pereira, Alexandra A.P. Mansur, Herman S. Mansur, Carmen Jerónimo, Susana R. Sousa, and Fernando J. Monteiro. Comprehensive Analysis of Secreted Protein, Acidic and Rich in Cysteine in Prostate Carcinogenesis: Development of a 3D Nanostructured Bone-Like Model. *Journal of Biomedical Nanotechnology*, 12(8):1667–1678, 2016. doi:10.1166/jbn.2016.2276.

[51] Susana Cruz-Neves, Nilza Ribeiro, Inês Graça, Carmen Jerónimo, Susana R. Sousa, and Fernando J. Monteiro. Behavior of prostate cancer cells in a nanohydroxyapatite/collagen bone scaffold. *Journal of Biomedical Materials Research Part A*, 105(7):2035–2046, 2017. doi:10.1002/jbm.a.36070.

[52] Terry L. Riss, Richard A. Moravec, Andrew L. Niles, Sarah Duellman, Hélène A. Benink, Tracy J. Worzella, and Lisa Minor. Cell Viability Assays. In *Assay Guidance Manual [Internet]*. Eli Lily & Company and the National Center for Advancing Translational Sciences, 2013. URL: https://www.ncbi.nlm.nih.gov/books/NBK144065/?report=reader.

[53] Bio-Rad Laboratories Inc. Real-Time PCR Applications Guide, 2006. URL: http://www.bio-rad.com/webroot/web/pdf/lsr/literature/Bulletin_5279.pdf.

[54] Joeri L. Aerts, Monica I. Gonzales, and Suzanne L. Topalian. Selection of appropriate control genes to assess expression of tumor antigens using real-time RT-PCR. *BioTechniques*, 36(1):84–91, 2004. doi:10.2144/04361ST04.

[55] Lynne V. Abruzzo, Kathleen Y. Lee, Alexandra Fuller, Alan Silverman, Michael J. Keating, L. Jeffrey Medeiros, and Kevin R. Coombes. Validation of oligonucleotide microarray data using microfluidic low-density arrays: a new statistical method to normalize real-time RT-PCR data. *BioTechniques*, 38(5):785–792, 2005. doi:10.2144/05385MT01.

[56] Kenneth J. Livak and Thomas D. Schmittgen. Analysis of Relative Gene Expression Data Using Real-Time Quantitative PCR and the $2^{-\Delta\Delta C_T}$ Method. *Methods*, 25(4):402–408, 2001. doi:10.1006/meth.2001.1262.

[57] Thomas D. Schmittgen and Kenneth J. Livak. Analyzing real-time PCR data by the comparative C_T method. *Nature Protocols*, 3:1101–1108, 2008. doi:10.1038/nprot.2008.73.

[58] Ellen C. Jensen. Real-Time Reverse Transcription Polymerase Chain Reaction to Measure mRNA: Use, Limitations, and Presentation of Results. *The Anatomical Record: Advances in Integrative Anatomy and Evolutionary Biology*, 295:1–3, 2012. doi:10.1002/ar.21487.

[59] Biswanath Maity, David Sheff, and Rory A. Fisher. Chapter 5 - Immunostaining: Detection of Signaling Protein Location in Tissues, Cells and Subcellular Compartments. *Laboratory Methods in Cell Biology*, 113:81–105, 2013. doi:10.1016/B978-0-12-407239-8.00005-7.

[60] Rongbin Ge, Zongwei Wang, Shulin Wu, Yangjia Zhuo, Aleksandar G. Otsetov, Chao Cai, Weide Zhong, Chin-Lee Wu, and Aria F. Olumi. Metformin represses cancer cells via alternate pathways in N-cadherin expressing vs. N-cadherin deficient cells. *Oncotarget*, 6(30):28973–28987, 2015. doi:10.18632/oncotarget.5023.

[61] Justin M. Drake, Garth Strohbehn, Thomas B. Bair, Jessica G. Moreland, and Michael D. Henry. ZEB1 Enhances Transendothelial Migration and Represses the Epithelial Phenotype of Prostate Cancer Cells. *Molecular Biology of the Cell*, 20(8):2207–2217, 2009. doi:10.1091/mbc.e08-10-1076.

[62] Xianghong Wang, Ming Tat Ling, Xin-Yuan Guan, Sai Wah Tsao, Hiu Wing Cheung, Davy Tak Lee, and Yong Chuan Wong. Identification of a novel function of TWIST, a bHLH protein, in the development of acquired taxol resistance in human cancer cells. *Oncogene*, 23:474–482, 2004. doi:10.1038/sj.onc.1207128.

[63] Azariyas A. Challa and Branko Stefanovic. A Novel Role of Vimentin Filaments: Binding and Stabilization of Collagen mRNAs. *Molecular and Cellular Biology*, 31(18):3773–3789, 2011. doi:10.1128/MCB.05263-11.

[64] Thermo Fisher Scientific Inc. CellTracker™ fluorescent probes: Product Information Sheet, 2018. URL: https://assets.thermofisher.com/TFS-Assets/LSG/manuals/MAN0001826_CellTracker_Probes_PI.pdf.

[65] Hiroko Sudo, Hiro-Ari Kodama, Yuji Amagai, Shigehisa Yamamoto, and Shiro Kasai. *In vitro* differentiation and calcification in a new clonal osteogenic cell line derived from newborn mouse calvaria. *Journal of Cell Biology*, 96(1):191–198, 1983. doi:10.1083/jcb.96.1.191.

[66] Sambad Sharma, Fei Xing, Yin Liu, Kerui Wu, Neveen Said, Radhika Pochampally, Yusuke Shiozawa, Hui-Kuan Lin, K. C. Balaji, and Kounosuke Watabe. Secreted Protein Acidic and Rich in Cysteine (SPARC) Mediates Metastatic Dormancy of Prostate Cancer in Bone. *The Journal of Biological Chemistry*, 291(37):19351–19363, 2016. doi:10.1074/jbc.M116.737379.

[67] Jindra Windrichova, Radka Fuchsova, Radek Kucera, Ondrej Topolcan, Ondrej Fiala, Jindrich Finek, Dagmar Slipkova, Marie Karlikova, and Jana Svobodova. Testing of a Novel Cancer Metastatic Multiplex Panel for the Detection of Bone-metastatic Disease - a Pilot Study. *Anticancer Research: International Journal of Cancer Research and Treatment*, 36(4):1973–1978, 2016. URL: http://ar.iiarjournals.org/content/36/4/1973.long.

[68] Jindra Windrichova, Radek Kucera, Radka Fuchsova, Ondrej Topolcan, Ondrej Fiala, Jana Svobodova, Jindrich Finek, and Dagmar Slipkova. An Assessment of Novel Biomarkers in Bone Metastatic Disease Using Multiplex Measurement and Multivariate Analysis. *Technology in Cancer Research & Treatment*, 17, 2018. doi:10.1177/1533033818807466.

[69] Qi Chen, Yuan-ting Yao, Huan Xu, Yan-bo Chen, Meng Gu, Zhi-kang Cai, and Zhong Wang. SPOCK1 promotes tumor growth and metastasis in human prostate cancer. *Drug Design, Development and Therapy*, 10:2311–2321, 2016. doi:10.2147/DDDT.S91321.

[70] Amalia Katafigioti, Ioannis Katafigiotis, Stavros Sfoungaristos, Christos Alamanis, Konstantinos Stravodimos, Ioannis Anastasiou, Eleni Roumelioti, Mordechai Duvdevani, and

Constantinos Constantinides. In the search of novel urine biomarkers for the early diagnosis of prostate cancer. Intracellular or secreted proteins as the target group? Where and how to search for possible biomarkers useful in the everyday clinical practice. *Archivio Italiano di Urologia e Andrologia*, 88(3):195–200, 2016. doi:10.4081/aiua.2016.3.195.

[71] Ilinca Georgescu, Robert J. Gooding, R. Christopher Doiron, Andrew Day, Shamini Selvarajah, Chris Davidson, David M. Berman, and Paul C. Park. Molecular characterization of Gleason patterns 3 and 4 prostate cancer using reverse Warburg effect-associated genes. *Cancer & Metabolism*, 4:8, 2016. doi:10.1186/s40170-016-0149-5.

[72] Shian-Ying Sung, Junn-Liang Chang, Kuan-Chou Chen, Shauh-Der Yeh, Yun-Ru Liu, Yen-Hao Su, Chia-Yen Hsueh, Leland W. K. Chung, and Chia-Ling Hsieh. Co-Targeting Prostate Cancer Epithelium and Bone Stroma by Human Osteonectin-Promoter-Mediated Suicide Gene Therapy Effectively Inhibits Androgen-Independent Prostate Cancer Growth. *PLOS ONE*, 11(4), 2016. doi:10.1371/journal.pone.0153350.

[73] Filippo Gagliardi, Ashwin Narayanan, and Pietro Mortini. SPARCL1 a novel player in cancer biology. *Critical Reviews in Oncology/Hematology*, 109:63–68, 2017. doi:10.1016/j.critrevonc.2016.11.013.

[74] Atsushi Okato, Takayuki Arai, Satoko Kojima, Keiichi Koshizuka, Yusaku Osako, Tetsuya Idichi, Akira Kurozumi, Yusuke Goto, Mayuko Kato, Yukio Naya, Tomohiko Ichikawa, and Naohiko Seki. Dual strands of pre-miR-150 (miR-150-5p and miR-150-3p) act as antitumor miRNAs targeting SPOCK1 in naïve and castration-resistant prostate cancer. *International Journal of Oncology*, 51(1):245–256, 2017. doi:10.3892/ijo.2017.4008.

[75] Yasutaka Yamada, Rika Nishikawa, Mayuko Kato, Atsushi Okato, Takayuki Arai, Satoko Kojima, Kazuto Yamazaki, Yukio Naya, Tomohiko Ichikawa, and Naohiko Seki. Regulation of HMGB3 by antitumor miR-205-5p inhibits cancer cell aggressiveness and is involved in prostate cancer pathogenesis. *Journal of Human Genetics*, 63(2):195–205, 2018. doi:10.1038/s10038-017-0371-1.

[76] Tieshi Liu, Xuefeng Qiu, Xiaozhi Zhao, Rong Yang, Huibo Lian, Feng Qu, Xiaogong Li, and Hongqian Guo. Hypermethylation of the SPARC promoter and its prognostic value for prostate cancer. *Oncology Reports*, 39(2):659–666, 2018. doi:10.3892/or.2017.6121.

[77] M. Yu Shkurnikov, D. V. Maltseva, E. N. Knyazev, and B. Ya Alekseev. Expression of Stroma Components in the Lymph Nodes Affected by Prostate Cancer Metastases. *Molecular Biology*, 52(5):701–706, 2018. doi:10.1134/S0026893318050126.

[78] Peng Hao, Bo Kang, Guoqing Yao, Wenqi Hao, and Feihong Ma. MicroRNA-211 suppresses prostate cancer proliferation by targeting SPARC. *Oncology Letters*, 15(4):4323–4329, 2018. doi:10.3892/ol.2018.7877.